AD-A118 950 INDUSTRIAL AND BIOMEDICAL SENSORS CORP WALTHAM MA F/G 6/11
DEVELOPMENT OF A HELIUM/CARBON DIOXIDE/HYDROGEN SENSOR SYSTEM F--ETC(U)
AUG 82 K W CHANG, S CHANG N00014-82-C-0134
UNCLASSIFIED NL

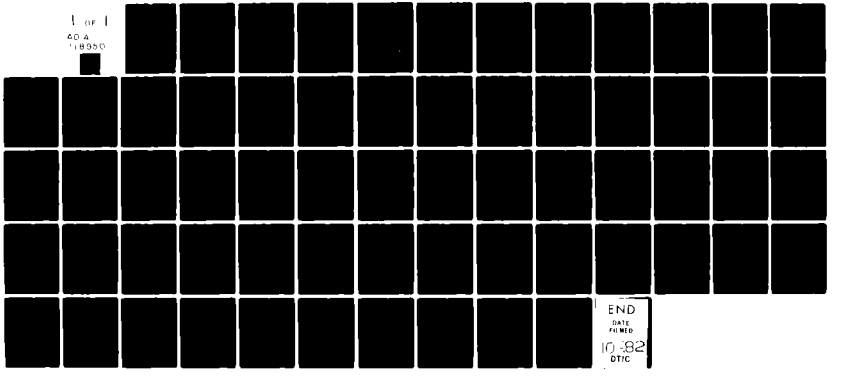

(12)

Report N00014-82-C-0134

DEVELOPMENT OF A HELIUM/CARBON DIOXIDE/HYDROGEN SENSOR SYSTEM FOR SCUBA

Kuo Wei Chang, Ph.D.
Sanlu Chang, M.S.
Industrial & Biomedical Sensors Corporation
1345 Main Street
Waltham, Massachusetts 02154

16 August 1982

Final Report for Period 1 January 1982 - 30 July 1982

Prepared for

OFFICE OF NAVAL RESEARCH
Department of the Navy
800 North Quincy Street
Arlington, Virginia 22217

Report N00014-82-C-0134

DEVELOPMENT OF A HELIUM/CARBON DIOXIDE/HYDROGEN SENSOR SYSTEM FOR SCUBA

Kuo Wei Chang, Ph.D.
Sanlu Chang, M.S.
Industrial & Biomedical Sensors Corporation
1345 Main Street
Waltham, Massachusetts 02154

16 August 1982

Final Report for Period 1 January 1982 - 30 July 1982

Prepared for

OFFICE OF NAVAL RESEARCH
Department of the Navy
800 North Quincy Street
Arlington, Virginia 22217

SECURITY CLASSIFICATION OF THIS PAGE (When Data Entered)

REPORT DOCUMENTATION PAGE		READ INSTRUCTIONS BEFORE COMPLETING FORM
1. REPORT NUMBER N00014-82-C-0134	2. GOVT ACCESSION NO. A118950	3. RECIPIENT'S CATALOG NUMBER
4. TITLE (and Subtitle) Development of a Helium/Carbon Dioxide/ Hydrogen Sensor System for SCUBA		5. TYPE OF REPORT & PERIOD COVERED Final Report for Period 1 January 1982-30 July 1982 6. PERFORMING ORG. REPORT NUMBER
7. AUTHOR(s) Kuo Wei Chang, Ph.D. and Sanlu Chang, M.S.		8. CONTRACT OR GRANT NUMBER(s) N00014-82-C-0134
9. PERFORMING ORGANIZATION NAME AND ADDRESS Industrial & Biomedical Sensors Corporation 1345 Main Street Waltham, Massachusetts 02154		10. PROGRAM ELEMENT, PROJECT, TASK AREA & WORK UNIT NUMBERS
11. CONTROLLING OFFICE NAME AND ADDRESS Office of Naval Research Department of the Navy 800 N. Quincy St., Arlington, VA 22217		12. REPORT DATE 16 August 1982 13. NUMBER OF PAGES
14. MONITORING AGENCY NAME & ADDRESS(if different from Controlling Office) DCASMA Boston, Code S2206A SCD-C 495 Summer Street Boston, Massachusetts 02210		15. SECURITY CLASS. (of this report) Unclassified 15a. DECLASSIFICATION/DOWNGRADING SCHEDULE
16. DISTRIBUTION STATEMENT (of this Report)		
17. DISTRIBUTION STATEMENT (of the abstract entered in Block 20, if different from Report)		
18. SUPPLEMENTARY NOTES		
19. KEY WORDS (Continue on reverse side if necessary and identify by block number) Helium Sensor, Carbon Dioxide Sensor, Hydrogen Sensor, Anion Exchange, SCUBA Diving, Piezoelectric Sensor, Diffusion, Speed of Sound, Membrane, Fuel Cell		

20. ABSTRACT (Continue on reverse side if necessary and identify by block number)

The feasibility of a Helium/Carbon Dioxide/Hydrogen sensor system for SCUBA diving has been investigated. The helium sensor is a piezoelectrically excited diaphragm with its acoustic characteristics related to the helium concentration. The carbon dioxide sensor is an enzymatic/electrolyte anion exchange cell operating in a diffusion controlled mode, where the cell current is proportional to the partial pressure of CO_2. The hydrogen sensor is a hydrogen/oxygen fuel cell operating in the hydrogen-diffusion-limited mode where the short

(continue on reverse side)

DD FORM 1 JAN 73 1473 EDITION OF 1 NOV 65 IS OBSOLETE

S/N 0102-LF-014-6601

SECURITY CLASSIFICATION OF THIS PAGE (When Data Entered)

20. circuit current is directly proportional to the hydrogen partial pressure.

Laboratory versions of various sensors have been fabricated and tested. Helium sensors based on frequency shift were found to be ineffective, whereas those based on amplitude attenuation measurement were feasible but impractical due to its requirement for depth correction. A more attractive ultrasonic speed-of-sound sensor which circumvents this problem has evolved from the current development. Also, the feasibility and practicality of the CO_2 and H_2 sensors has been demonstrated. These sensors were found to be compact, rugged, sensitive, fast responding and linear within the range of interest. Most importantly, these sensors were designed to come under membrane diffusion control so that their output signals are more reliable and stable on a long term basis.

SUMMARY

The feasibility of a Helium/Carbon Dioxide/Hydrogen sensor system for SCUBA diving has been investigated. The helium sensor is a piezoelectrically excited diaphragm with its acoustic characteristics related to the helium concentration. The carbon dioxide sensor is an enzymatic/electrolyte anion exchange cell operating in a diffusion controlled mode, where the cell current is proportional to the partial pressure of CO_2. The hydrogen sensor is a hydrogen/oxygen fuel cell operating in the hydrogen-diffusion-limited mode where the short circuit current is directly proportional to the hydrogen partial pressure.

Laboratory versions of various sensors have been fabricated and tested. Helium sensors based on frequency shift were found to be ineffective, whereas those based on amplitude attenuation measurement were feasible but impractical due to its requirement for depth correction. A more attractive ultrasonic speed-of-sound sensor which circumvents this problem has evolved from the current development. Also, the feasibility and practicality of the CO_2 and H_2 sensors has been demonstrated. These sensors were found to be compact, rugged, sensitive, fast responding and linear within the range of interest. Most importantly, these sensors were designed to come under membrane diffusion control so that their output signals are more reliable and stable on a long term basis.

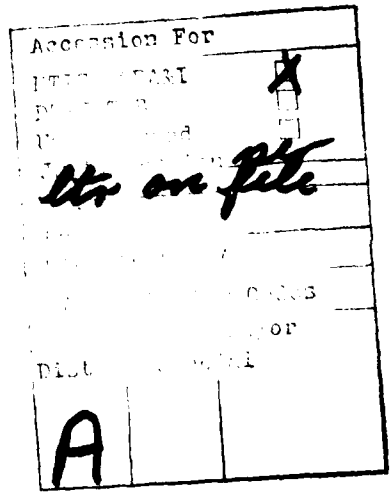

TABLE OF CONTENTS

1.0 INTRODUCTION

This FINAL REPORT is a summary of a six-month program to determine the feasibility of a Helium/Carbon Dioxide/Hydrogen sensor system for underwater gas analysis in SCUBA.

In deep, long dives, helium is commonly used to replace nitrogen in the breathing gas. For rebreather type SCUBA systems, helium can be used only if an accurate helium sensor is available to monitor and maintain the proper gas mixture. Because helium is an inert noble gas, its detection is difficult and can be done only with bulky equipment such as a spectroscope.

The helium sensor under current development is a piezo-electrically or electromagnetically excited reed with its acoustic characteristics related to the concentration of helium. It is built on a commonly observed phenomenon that when helium is breathed, the human vocal cords vibrate differently, resulting in a "Mickey Mouse" type voice. For SCUBA diving, the sensor must operate under varying hydrostatic pressure conditions with a helium concentration ranging from 79% (balance O_2) at sea level to almost 100% at great depths.

Two versions of the proposed helium sensors, one based on frequency-shift and the other based on amplitude detection, have been evaluated. The method involving amplitude measurement was found to be more reliable, easier to implement and more sensitive. Other salient features include long term stability, reliability, ruggedness and small size.

The principal drawback of the amplitude-detection helium sensor lies in its sensitivity to hydrostatic pressure. As a result, different calibration curves for different depths must be used. An alternate method involving speed of sound measurement is also described in this REPORT. Based on theoretical considerations, the speed of sound is a function of mole fraction, γ (ratio of specific heats) and molecular weight of the component gases and is independent of pressure and density, and depth. A better method of helium measurement based on the speed of sound variation has been described.

Carbon dioxide toxicity is a frequently encountered problem when a rebreathing type SCUBA system is used. Like helium, carbon dioxide is also fairly inert and is very difficult to measure. Conventional CO_2 sensors

use a pH probe to measure the concentration of hydrogen ions produced when CO_2 dissolves in water to form carbonic acid. The most serious problem associated with conventional CO_2 sensors is its tendency to drift. Besides, the glass electrode of a pH probe has high output impedance (larger than 200 Mega Ohm) which presents an almost insurmountable sealing and insulating problem in underwater applications. A stable, rugged CO_2 sensor suitable for diving apparatus is urgently needed.

The carbon dioxide sensor under current development is an enzymatic/electrolytic anion exchange cell operating in a diffusion controlled mode where the cell current is proportional to the partial pressure of CO_2. The sensor is compact, fast responding, rugged, sensitive, linear within the range of interest and has low offset current. The sensor is potentially stable and long term stability over a 9-day test period has been established. With further refinement, the proposed sensor may indeed be useful for CO_2 monitoring in a rebreather SCUBA system. It may even be utilized in respiratory CO_2 measurement if the response time can be improved further through judicious selection of an optimum membrane material.

Being a lighter gas, hydrogen and its use allows the diver to go into greater depths than helium. Hydrogen is a very reactive gas and its measurement is less difficult. The hydrogen sensor under current development is a fuel cell operating in the hydrogen-diffusion-limited mode where the short circuit current is directly proportional to the partial pressure of H_2. Similar to the helium sensor, the range of interest for hydrogen measurement is between 79% H_2 (balance O_2) and 100% H_2, corresponding to the gas mixture at sea level and at great depths, respectively.

To date, only laboratory versions of various sensors have been fabricated and tested. The feasibility and practicality of each sensor has been evaluated and the results are given in sections to follow. More detailed sensor designs envisioned for ultimate utilization in SCUBA diving have also been advanced.

2.0 HELIUM SENSOR

It is a commonly observed phenomenon that when helium is breathed, the human vocal cords vibrate differently, resulting in a "Mickey Mouse" type voice. The feasibility of utilizing this effect in the detection of helium is explored in this section.

2.1 Preliminary Study

A simple experiment has been performed to study the effect of helium on a vibrating ceramic crystal. The experimental set-up used is schematically shown in Figure 1. The piezoelectric audio transducer was driven by a low output-impedance sinewave generator. A biased electret microphone facing the audio transducer was used to monitor the transmitted sound wave. The frequency and amplitude of the sound wave can be read directly from the oscilloscope.

The frequency and amplitude of the sinewave generator was so selected that the sound signal picked up by the microphone was maximized without waveform distortion and signal saturation. For the piezoelectric cystal used, the frequency at the strongest resonance was 2.8 KHz and the signal received was 1 Volt peak-to-peak. As soon as helium was introduced, the sound volume was markedly reduced, and the signal detected by the microphone dropped to 0.17 Volt peak-to-peak. The frequency dial of the sinewave generator was then readjusted for maximum output. The new resonant frequency was at 2.65 KHz and the amplitude was 0.2 Volt peak-to-peak. After the helium was shut off, the sound volume increased and the reading on the oscilloscope became 0.6 Volt peak-to-peak at 2.65 KHz. Again, after re-adjusting the frequency dial of the sinewave generator, the reading returned to 1 Volt peak-to-peak with a frequency of 2.8 KHz at resonance.

After the helium was shut off, the rate of recovery of the amplitude and the sound volume were found to depend on how fast the room air was allowed to enter. Closing the vent at any point in time caused the amplitude to remain constant indefinitely.

The afore-mentioned simple experiment clearly shows that replacement of air by helium causes both a shift in the resonant frequency of the piezoelectric transmitter and a considerable attenuation of the acoustic signal detected

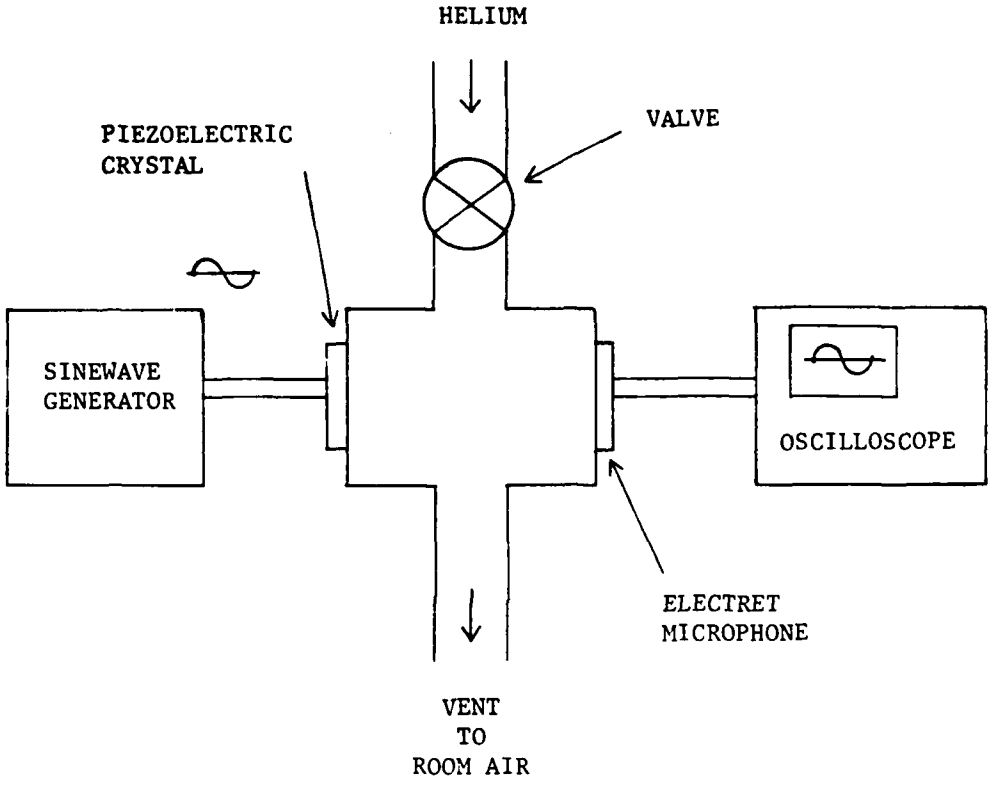

FIGURE 1. EXPERIMENTAL SET-UP FOR PRELIMINARY STUDY OF HELIUM SENSOR.

by the microphone. Therefore, two versions of the helium sensor can be devised; one based on frequency-shift while the other on amplitude change.

2.2 Frequency-Shift Helium Sensor

Helium, being a lighter gas, offers less resistance to a vibrating reed or diaphragm. This reduction in the loading effect can alter the natural resonant frequency of the oscillating system.

A design of the frequency-shift helium sensor is illustrated in Figure 2. A piezoelectric ceramic crystal bender acting as the sensing crystal is flanked by an identical reference crystal sealed in a metal bellow pre-filled with a suitable gas reference such as helium. The function of the metal bellow is to impart the same ambient pressure to the reference crystal. The beat frequency between the two crystal oscillators represents the frequency-shift as a result of changes in the ambient helium concentration.

The frequency response of crystals to helium has been studied using the simple setup shown in Figure 1. The piezoelectric ceramic material used for crystal oscillator construction were obtained from Piezo Products Division, Gulton Industries, Inc., Metuchen, New Jersey and Projects Unlimited, Inc., Dayton, Ohio. In the audible range (below 18 KHz), the crystal oscillator is composed of a circular brass diaphragm with a piezoelectric element bonded to its surface. In the ultrasonic range, the crystal generators generally consist of square and rectangular bimorph ceramic bender elements.

It has been found that the frequency-shift is completely dictated by sensor construction. For crystals operating in the ultrasonic range, the frequency-shift is, in general, minute or undetectable when helium is introduced. This is perhaps due to the fact that the resistance exerted by the gas medium on the crystal represents only a fraction of the total crystal loading. Therefore, a reduction in resistance due to the presence of helium has a negligible effect on the resonant frequency.

For crystals with a metal diaphragm which operate in the low frequency audible range, the resistance due to the surrounding gas medium can become a significant part of the total crystal loading. As a result, substantial frequency-shift can be detected on some crystal oscillators, especially

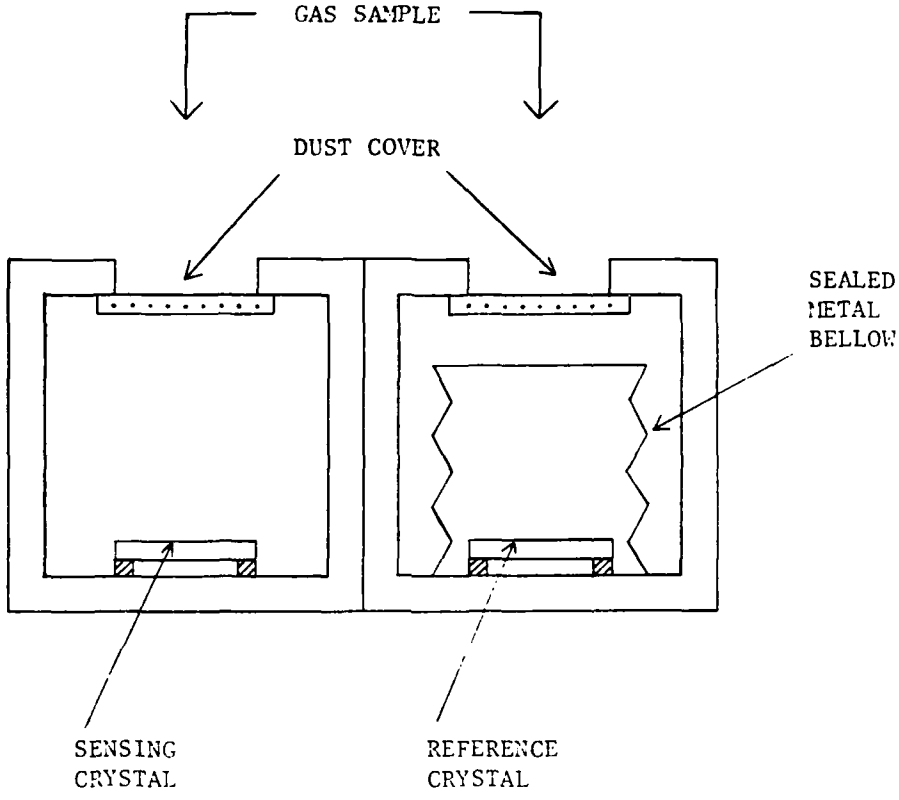

FIGURE 2. SCHEMATIC DIAGRAM SHOWING A DESIGN OF THE FREQUENCY SHIFT HELIUM SENSOR.

those with a relatively large, thin metal diaphragm. The magnitude of frequency-shift of a given crystal can be augmented by increasing the power level and amplitude of oscillation. Variations of frequency-shift with helium concentration for two such crystals are given in Figures 3 and 4.

A critical review of performance has led us to the conclusion that the frequency-shift helium sensor is not effective nor feasible for helium measurement in SCUBA diving. The reasons are:

1) In the range of interest where the helium concentration is between 79% and 100%, the frequency-shift has a saturation effect (Figure 3) and is not senstive to helium concentration. Although the crystal operating at higher frequency (Figure 4) does have enough sensitivity in the range of interest, its use is impractical largely due to the presence of an audible tone which may prove to be too annoying for the diver. In addition, spurious sounds which are common in a gas flow system, may cause serious interference with the frequency-shift measurement at these low frequencies.

2) Accurate and reliable frequency-shift measurement is difficult due to the inferior "Q" factor of piezoelectric oscillators at low frequency.

3) In underwater application, the gas becomes denser with depth, and the loading on the crystal is increased. Therefore, different calibration curves for different depths are required.

4) In order to obtain a significant frequency-shift, the crystal is normally overdriven. Degradation of the crystal and signal drift may prove to be prohibitive.

Therefore, while the resonant frequency of the human vocal cord is sensitive to the helium concentration, the same effect cannot be effectively duplicated in a mechanical crystal oscillator system.

2.3 Amplitude-Detection Helium Sensor

The design of an amplitude-detection helium sensor is illustrated in

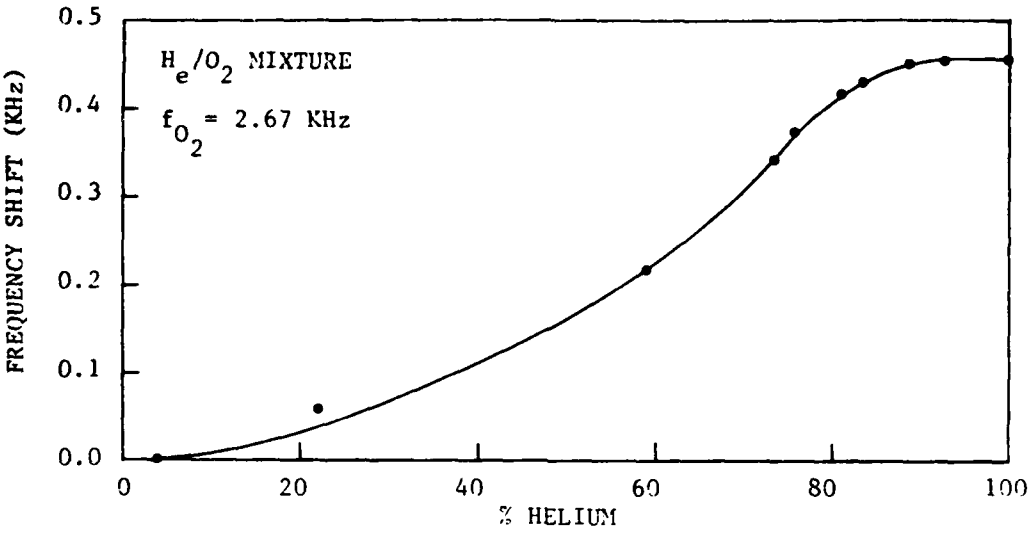

FIGURE 3. FREQUENCY SHIFT VERSUS HELIUM CONCENTRATION FOR SENSOR H-1.

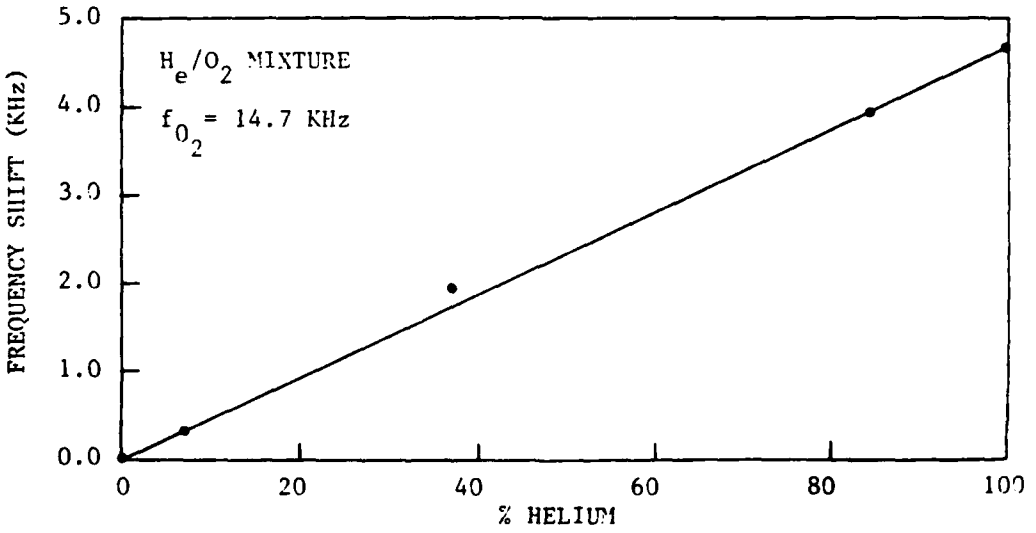

FIGURE 4. FREQUENCY SHIFT VERSUS HELIUM CONCENTRATION FOR SENSOR H-2.

Figure 5. A crystal oscillator is mounted directly opposite a tiny electret microphone. The piezoelectric oscillator is so constructed that the frequency-shift due to the presence of helium is minimized. The crystal is driven by a simple sinewave generator circuit at a constant frequency at or near resonance. The voltage output of the sinewave generator will be kept low so that the crystal is only lightly excited. The crystal can also be excited by a standard resonant circuit (a two-stage feedback or a Pierce oscillator). The output of the microphone can be tuned at roughly the same operating frequency to reject spurious noises (i.e, by means of filters).

The dynamic response of various crystal oscillators in an O_2-He gas mixture has been measured. Typical performance of crystals in the audible and near ultrasonic ranges are given in Figures 6 and 7, respectively. The measurements were taken at 1 atm using a flow system composed of flowmeters, check valves, flow barriers and a mixing chamber. The distance ℓ (Figure 5) between the crystal and the microphone is approximately 1.6 cm. The electret microphone used was manufactured by Knowles Electronics, Inc., Franklin Park, Illinois (Model BT-1759). The microphone is 0.79 cm long, 0.56 cm wide and 0.23 cm thick and has a frequency response extending to 20 KHz, approximately.

The performance data presented in Figures 6 and 7 clearly indicated that while the amplitude-detection helium sensor may be effective over a wide dynamic range, it is, however, quite ineffective for measurement over the narrow range of interest between 79% and 100% helium. Further improvement of the sensor design is therefore indicated. Ideally we want to expand the response curve in such a way that at 79% He and 21% O_2, the signal is as large as the signal corresponding to 100% O_2.

In anticipation of possible standing wave interaction, an attempt was made to optimize the separation between the crystal and the microphone (i.e., distance ℓ in Figure 5). The effect of spatial variation on sensor response was shown in Figure 8. At a distance of approximately 1.5 cm, the amplitude is most sensitive to helium within the concentration range of interest. The data given in Figure 8 were obtained using pre-mixed gases supplied by Airco, Inc. of Riverton, New Jersey. The contents of the gases were factory analyzed by means of gas chromatography.

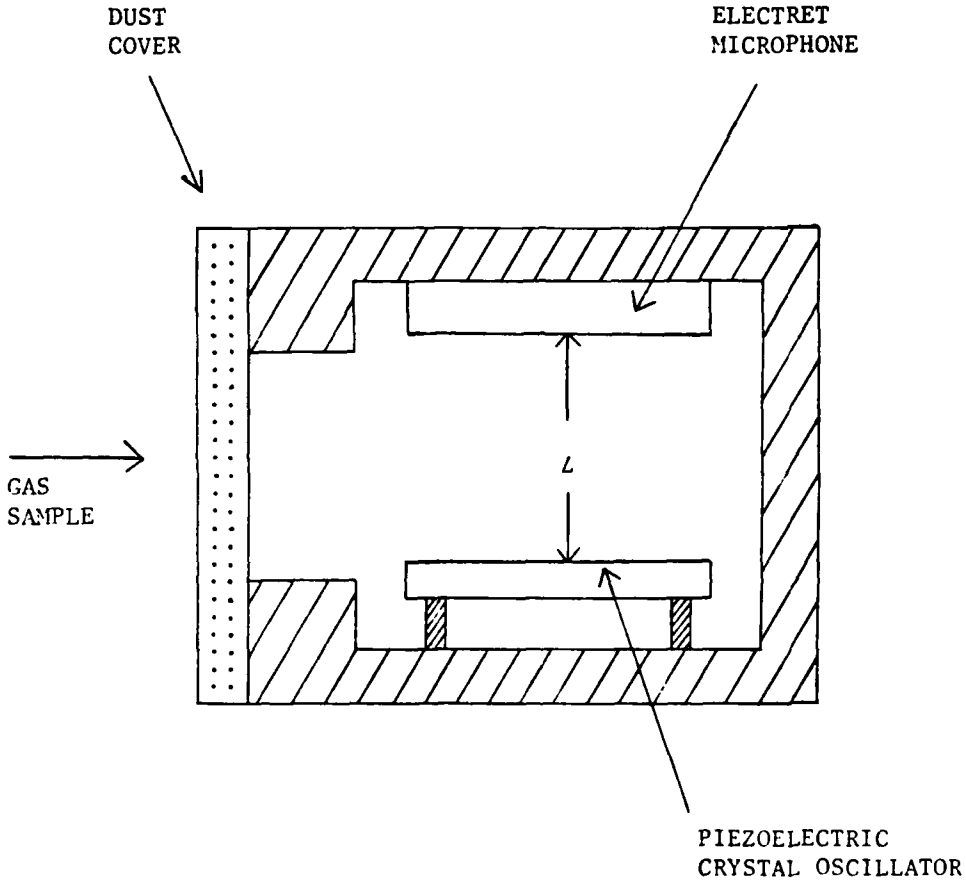

FIGURE 5. SCHEMATIC DIAGRAM OF AN AMPLITUDE-DETECTION HELIUM SENSOR.

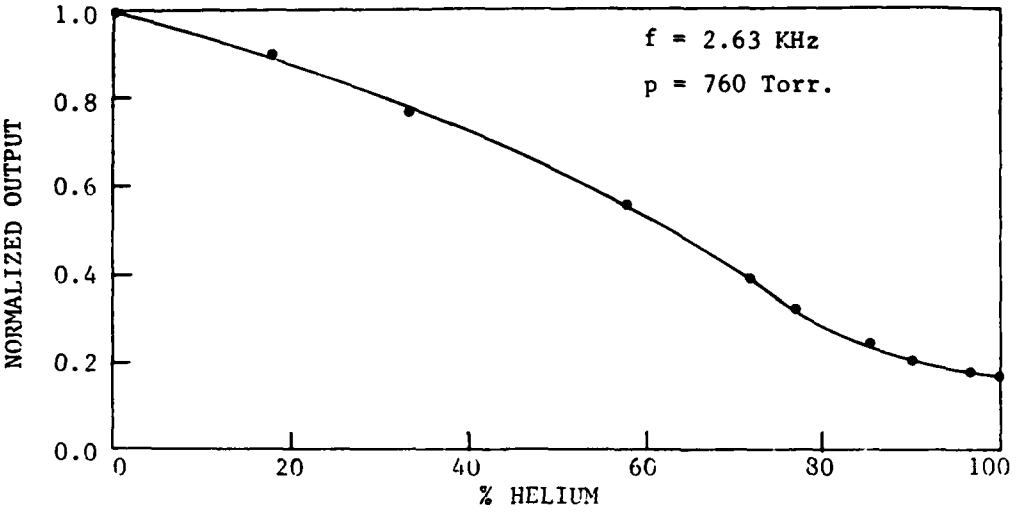

FIGURE 6. AMPLITUDE ATTENUATION VERSUS HELIUM CONCENTRATION FOR SENSOR H-3.

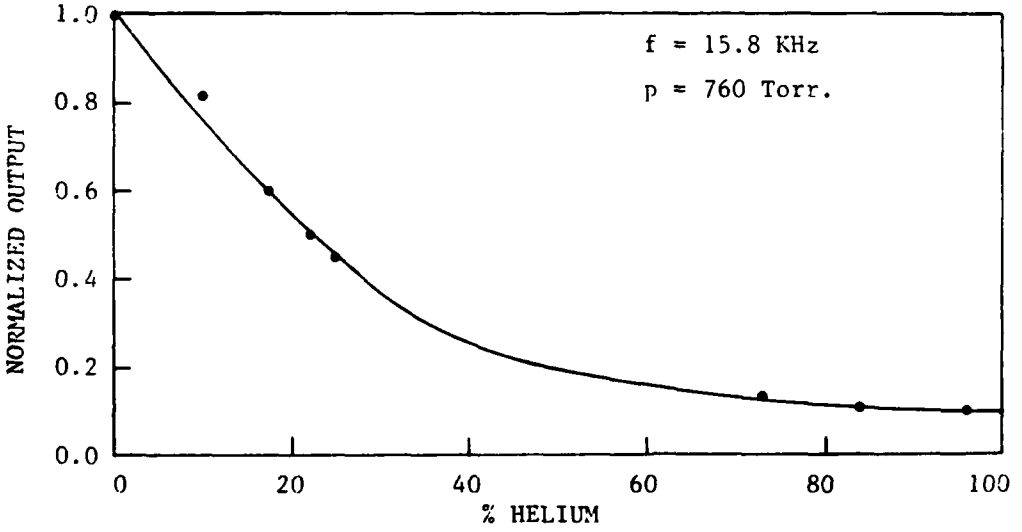

FIGURE 7. AMPLITUDE ATTENUATION VERSUS HELIUM CONCENTRATION FOR SENSOR H-4.

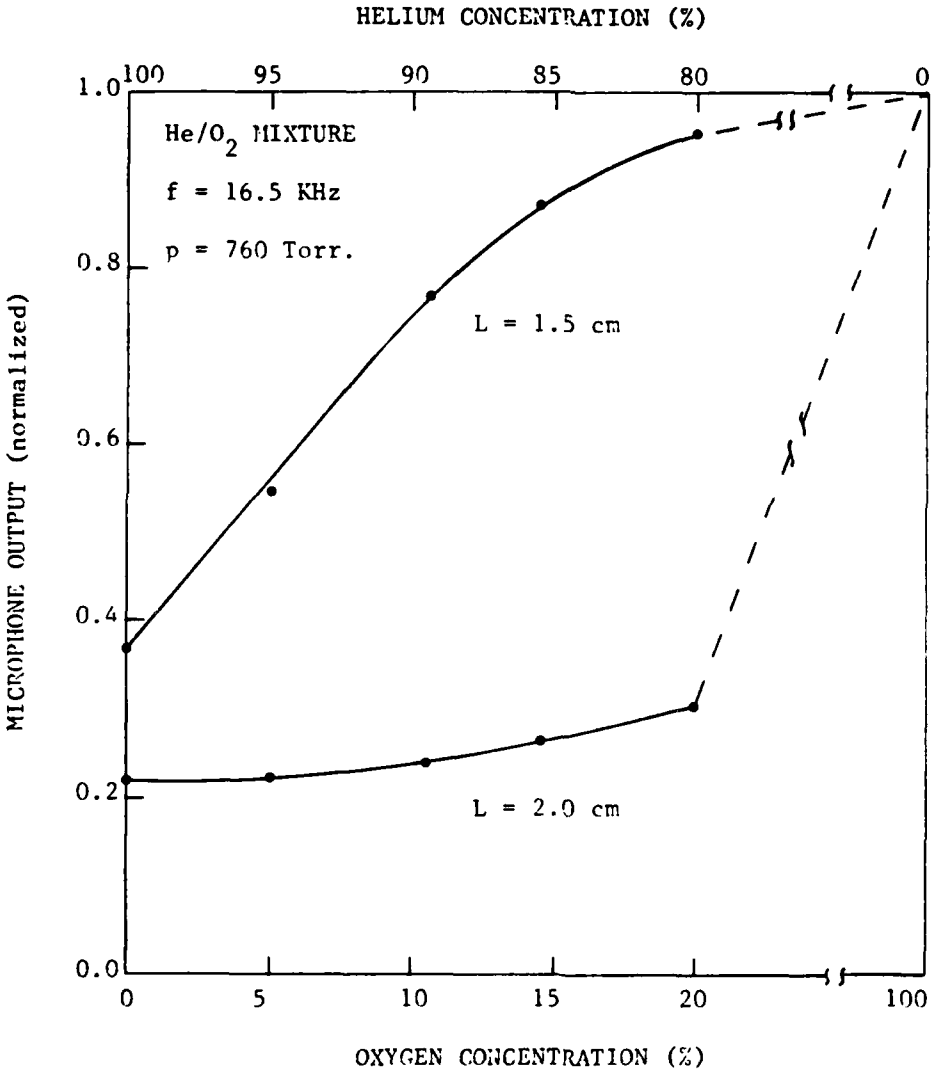

FIGURE 8. EFFECT OF CRYSTAL-MICROPHONE SEPARATION ON SENSOR PERFORMANCE.

The mechanisms responsible for amplitude detection are very complex. Volumetric absorption due to frictional dissipation is obviously minuscule. The observed signal attenuation in the presence of helium is partly due to a reduction in the coupling factor between the crystal and the gas medium and most importantly, due to a complex standing wave phenomenon caused by the drastic increase in speed of sound.

As the mass density is reduced upon introduction of helium, the acoustic energy emitted or transmitted by the vibrating diaphragm is also reduced. For an ideal, harmonically driven plate or disc, the sound wave generated is directly proportional to the mass density (Ref. 1-3). In the case of piezoelectric oscillators, driven either by a constant amplitude (voltage) sinewave generator or a constant voltage resonant circuit, the forcing function or the acceleration of the diaphragm also varies with the gas loading (i.e., the mass density). Therefore, the emitted acoustic energy is a complex function of mass density and properties of the crystal.

The effect of mass density on the signal detected by the microphone (Figure 5) has been studied and the results for pure oxygen and helium are presented in Figure 9. For the same gas, as pressure increases, the mass density also increases proportionally, resulting in a higher coupling factor and a higher signal. However, doubling the pressure and density does not result in a concomitant two-fold increase in signal, as in the case of a constant amplitude, harmonically driven classical oscillator.

The most important factor responsible for the observed amplitude variation lies in wave interaction. To explain this effect, we shall digress to certain idealized cases. When the microphone is located far from the crystal, the oscillator in effect resembles a point source and the signal drop-off is largely due to geometric factors. A sensor so located is expected to be insensitive to helium concentration. The criteria for "near" and "far" is defined in terms of the wave length:

$$\frac{L}{\lambda} \lesssim 1 \qquad \text{near} \qquad (1)$$

$$\frac{L}{\lambda} >> 1 \qquad \text{far} \qquad (2)$$

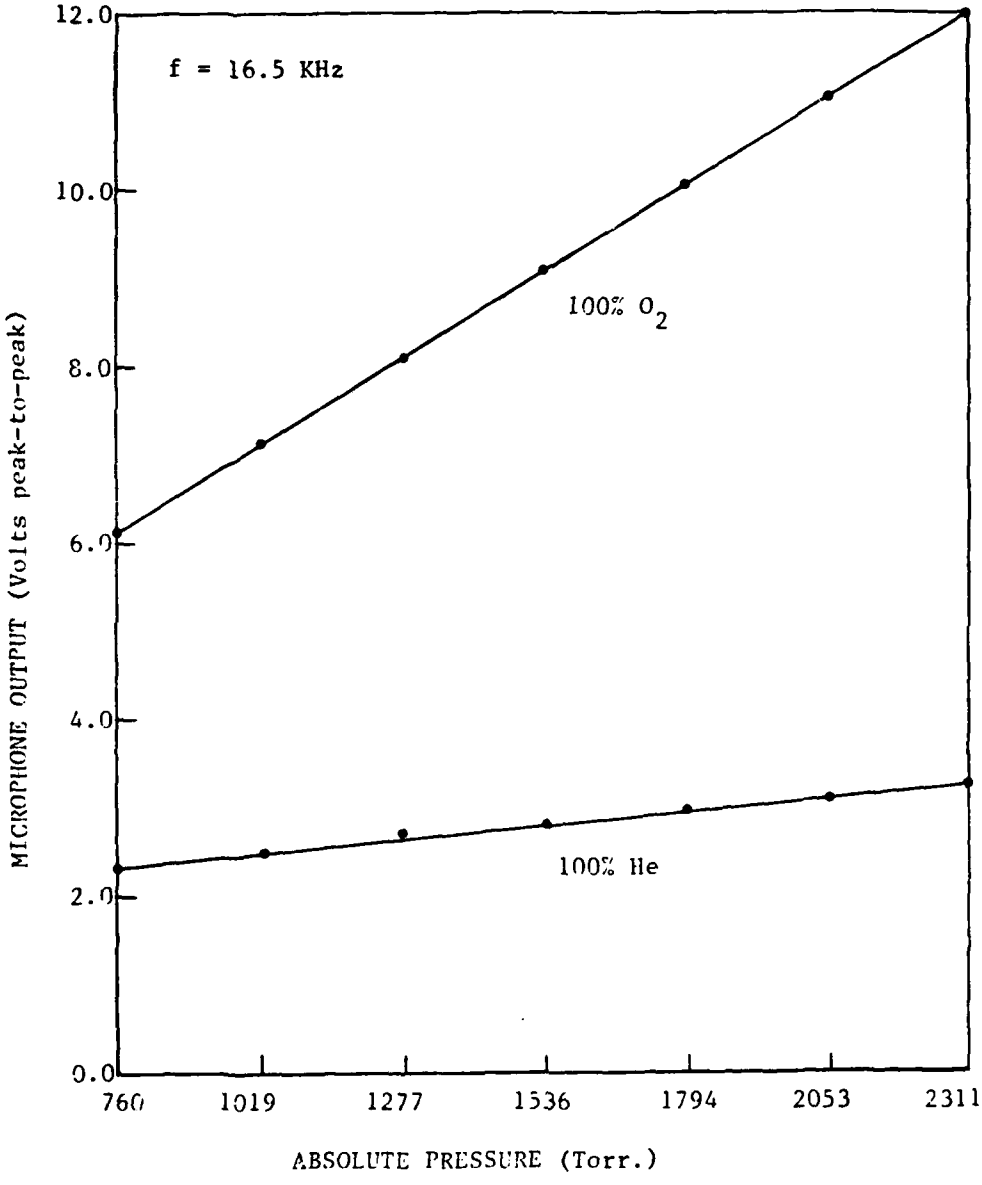

FIGURE 9. EFFECT OF PRESSURE ON MICROPHONE OUTPUT FOR OXYGEN AND HELIUM.

Here ℓ is the distance and λ, the wave length given by

$$\lambda = \frac{c}{f} \qquad (3)$$

where c is the speed of sound and f, the frequency. For the sensor system shown in Figure 5 where the distance is constant, the microphone becomes effectively farther and farther as the frequency is increased. Therefore, the sensor would be less sensitive to helium as frequency increases. Measurements have confirmed that high frequency, ultrasonic crystal benders are insensitive, and some even impervious, to the presence of helium at any concentration.

The speed of sound for oxygen and helium at room temperature (298°K) is 329 m/sec and 1020 m/sec, respectively. For a crystal oscillating at 16.5 KHz which is most suitable for the present application, the wavelength is approximately 2 cm in oxygen and 6 cm in helium. Hence, the wave interaction involved is of the "near" field type satisfying the criterium $\ell/\lambda \lesssim 1$ with ℓ in the range between 1 to 3 cm.

For near field interaction where the diameter of the diaphragm is larger than the microphone, the wave problem can be reduced to one involving a harmonically pulsating plane, at least from a qualitative point of view. The solution for one dimensional wave equation yields a standing wave pattern such as those shown in Figure 10 with nodal points at quarter and three-quarter wavelength. The standing wave envelope shown in Figure 10b represents the amplitude of oscillation at each spatial point. If a microphone were to place at x = 1 cm, it would register a sinusoidal signal with a peak-to-peak reading equal to 2A. If the microphone were to move closer to the pulsating plane, the peak-to-peak reading would decrease until finally at x = 0.5 cm where no signal would be registered. In the case of helium, the same phenomenon prevails with the exception of a longer wave length (Figure 10c).

The curves in Figure 10b and c are combined together in Figure 11. Referring to Figure 11, one can see that if a microphone is placed at $X = L_1$, the amplitude of detected signal will vary from point C to D as the gas

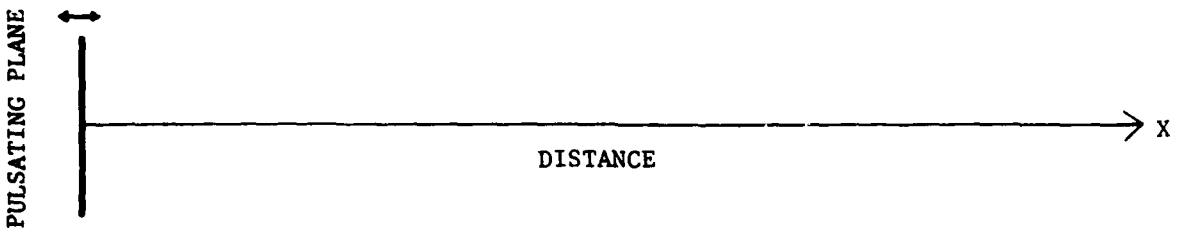

FIGURE 10a. PULSATING PLANE IN ONE DIMENSIONAL SPACE.

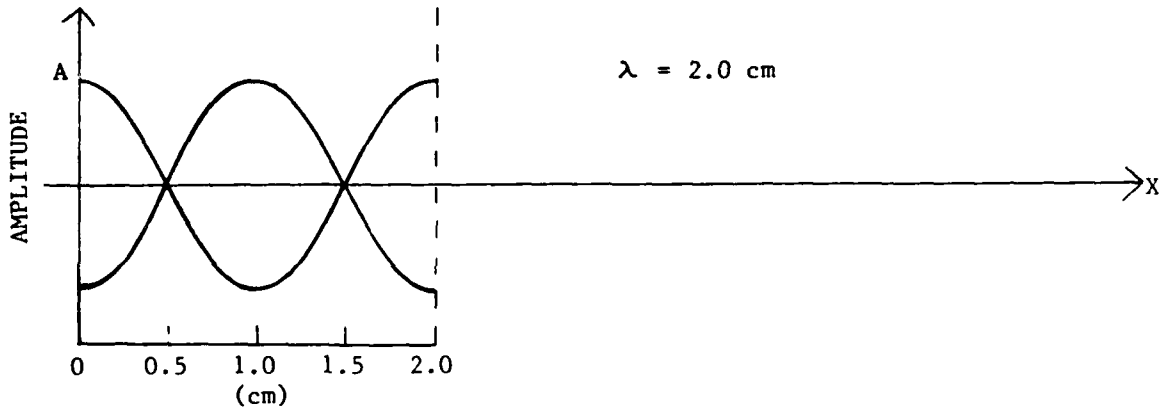

FIGURE 10b. ENVELOP OF STANDING WAVE IN OXYGEN.

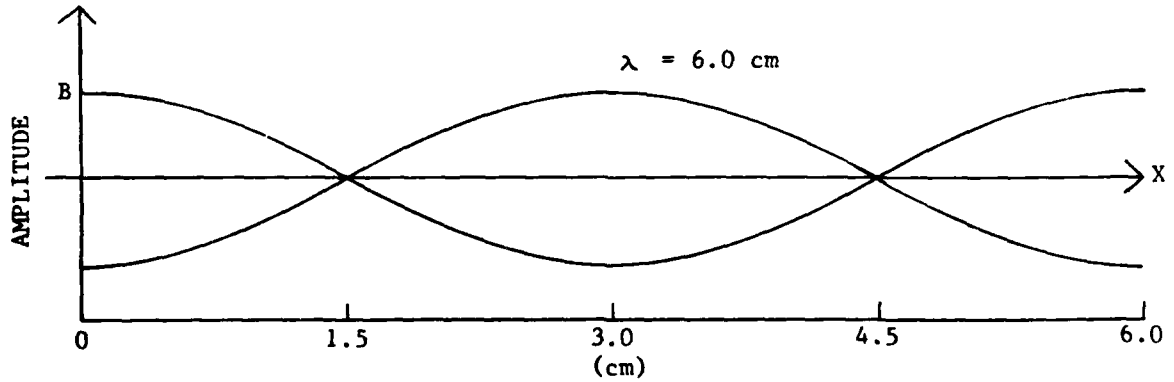

FIGURE 10c. ENVELOP OF STANDING WAVE IN HELIUM.

FIGURE 10. ILLUSTRATION OF WAVE LENGTH INTERACTION.

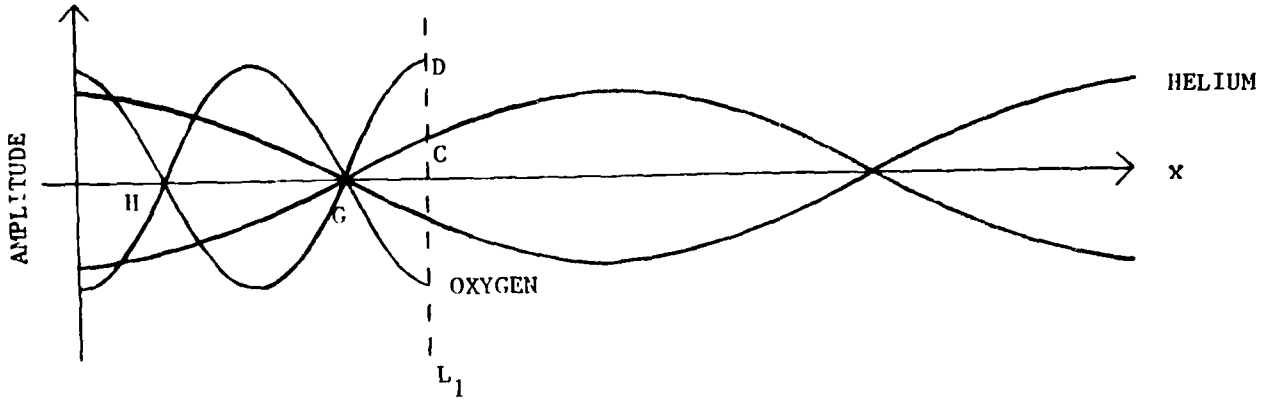

FIGURE 11. COMPOSIT DRAWING OF WAVE ENVELOPES.

mixture is varied from 100% helium to 100% oxygen, whereas the first nodal point corresponding to each gas mixture will move in the -x direction from point G (100% He) to point H (100% O_2). Therefore, it becomes obvious that if one wishes to measure low concentrations of oxygen (i.e., high concentration of helium such as the range of interest for SCUBA diving), one would place the microphone at or near the nodal point G. Conversely, one would place the microphone near the nodal point H if low concentrations of helium are to be measured. At point G, the signal will rise from zero, reach a peak and then fall to zero as the He concentration varies from 100% to 0%.

The simple qualitative description of the wave length effect was given to show how placement of the microphone can drastically affect the sensor response (Figure 8). In reality, the situation is extremely more complicated due to three-dimensionality, wave reflection off sensor cell walls and a host of other factors. It also appears that the sensor should be designed with spatial tuning capability for optimization of sensitivity and performance.

The performance of a typical sensor under different hydrostatic pressure conditions has been studied and results are summarized in Figure 12. Again, pre-mixed and analyzed gases were used in the test. It appears inevitable that different calibration curves for different depths will be required.

A variety of tests designed to elucidate the underlying principle and to characterize the sensor performance have also been conducted. A summary of essential findings are given as follows:

1) Electro-mechanical, magnetic-coil type oscillatore composed of a ferritecore and a bi-metallic diaphragm can be used to replace the piezoelectric oscillator in the helium sensor. The advantage lies in ruggedness, small diameter (1.3 cm), and unlike their crystalline counterparts, there is no epoxy bonding, no wire leading to vibrating crystal (and the attendant metallic fatigue and breakage problem), and no long term degradation due to repeated flexure. Height (0.5 cm) and weight (3.5 gm) are perhaps some of the drawbacks of such oscillators. For the helium sensor based on amplitude measurement, a stable, predictable generator

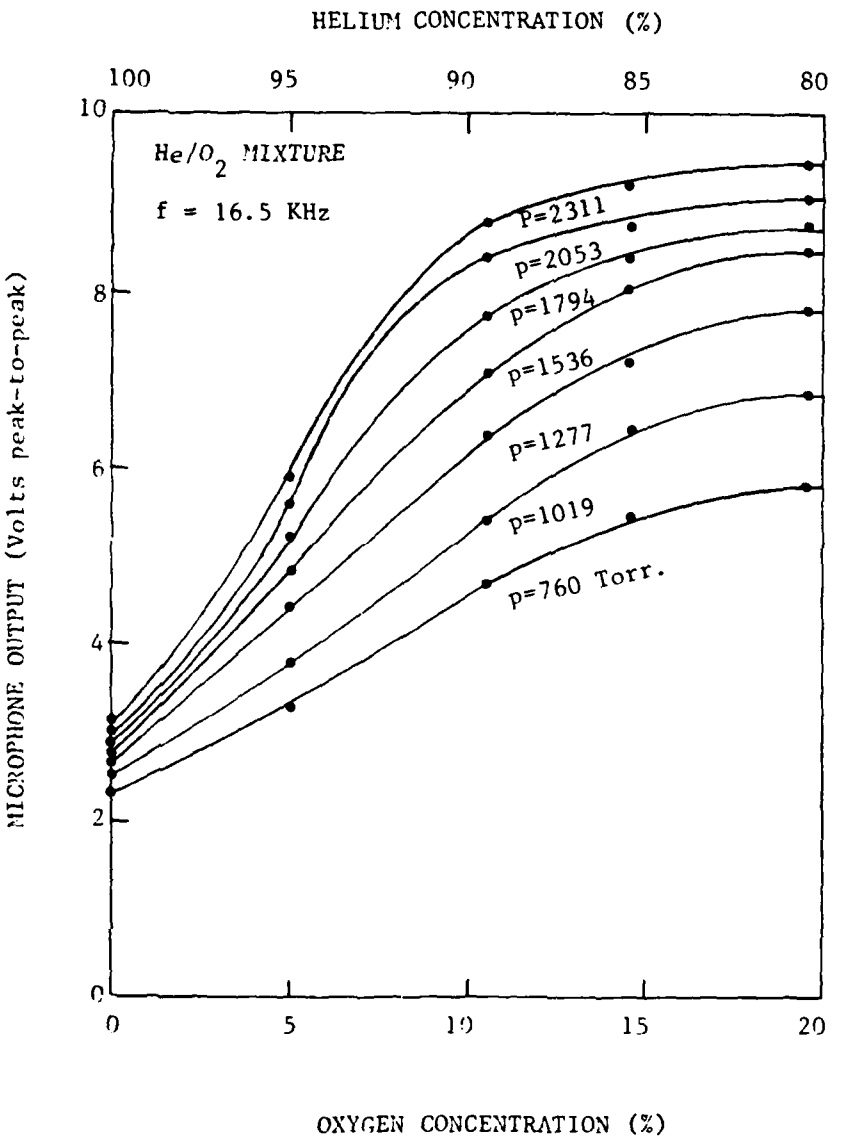

FIGURE 12. HELIUM SENSOR CALIBRATION CURVE UNDER DIFFERENT HYDROSTATIC PRESSURE CONDITIONS.

such as the afore-mentioned electro-mechanical oscillator is favored.

2) The response time of the sensor system shown in Figure 5 appears to be almost as fast as the filling time within the sensor cavity. Therefore, it can be used for respiration measurement especially in a flow through type design.

3) The sensor response is highly reproducible and there was no noticeable drift when tested with a pre-mixed gas mixture (10.4% oxygen and balance helium) over an 8-hour measurement period.

4) The helium sensor is non-specific. Because it is built on the great disparity in molecular weight, qualitatively similar results were obtained when tested with pre-mixed hydrogen-argon gas ranging from 100% H_2 to 79.8% H_2 (argon was used to replace oxygen for safety reasons).

Finally, the performance of the amplitude-detection helium sensor can be summarized as follows:

1) The sensor can be designed to fit any segment of the dynamic measurement range between 0 and 100% He by varying the location of the microphone.

2) The sensor can be used either for automatic mixture control or for respiration gas analysis.

3) The sensor has a major drawback. It is sensitive to hydrostatic pressure and therefore, different calibration curves exist for different depths. The hydrostatic pressure effect can be compensated for only by empirical means (or by a micro-processor based system).

To circumvent the serious drawback just mentioned, an ultrasonic helium sensor has been devised, which will be the subject matter of the following section. This alternate helium sensor is based on the speed of sound measurement, and is expected to be completely insensitive to the hydrostatic pressure and depth. In hindsight, this method should have been the approach of choice in the first place.

2.4 Ultrasonic Helium Sensor

The helium sensor reported in the previous section has a serious drawback relating to high sensitivity to hydrostatic pressure. The sensor described in this section is based on the speed of sound measurement and it is potentially immune to changes in the hydrostatic pressure.

Although the previous sensor is based on amplitude measurement, the observed variations in amplitude are predominately due to changes in the speed of sound reflected in the changes of wave length. Since the speed of sound is responsible for basic interaction mechanisms, its direct measurement is indicated.

Based on the small perturbation theory of acoustic wave, the speed of sound, c, can be expressed in terms of various related physical parameters:

$$c = \sqrt{\frac{dP}{d\rho}} = \sqrt{\gamma \frac{P}{\rho}} = \sqrt{\frac{\gamma RT}{M}} \qquad (4)$$

Where
- P = gas pressure which is equal to hydrostatic pressure in diving
- ρ = mass density
- γ = ratio of specific heat
- R = universal gas constant
- M = molecular weight
- T = temperature

It is apparent from eq.(4) that the speed of sound is only a function of gas temperature and is independent of the hydrostatic pressure and depth. Values of γ, M and the speed of sound at room temperature (298° K) for various gases are summarized in Table 1.

TABLE 1

Properties of Gases Used in SCUBA Diving

Gas	γ	M	C (cm/sec)
O_2	$\frac{7}{5}$	32	3.29×10^4
He	$\frac{5}{3}$	4	10.7×10^4

con't

Gas	γ	M	C (cm/sec)
H_2O	$\frac{4}{3}$	18	4.28×10^4
CO_2	$\frac{7}{5}$	44	2.81×10^4
H_2	$\frac{7}{5}$	2	13.2×10^4

Following a simple derivation, we have the following expression for the speed of sound in a multi-component gas mixture:

$$C = \sqrt{\frac{\sum_a n_a \gamma_a}{\sum_a n_a M_a} RT} \qquad (5)$$

where n is the mole fraction and the subscript "a" denotes the component gas in the mixture. Eq.(5) is expected to remain valid for the temperature and pressure ranges relevant to SCUBA diving.

The speed of sound in a two-component He/O_2 gas mixture has been calculated and the results are given in Figure 13. It is apparent that the percentage concentration of a He/O_2 mixture can effectively be determined through measurement of the speed of sound.

The speed of sound can be determined by the transit time principle illustrated in Figure 14. A piezoelectric crystal driven by a gated oscillator circuit emits a brief burst of ultrasound, which propagates through the gas mixture. Because the same crystal is used for both transmitting and receiving, a smooth reflecting wall is provided. The crystal receives both the strong driving signal and the weak echo sequentially in time. The transit time and the corresponding speed of sound can be obtained with a simple circuitry in real time. The process is then repeated at a fixed, high rate, providing a practically continuous measurement of the helium concentration.

In the case of SCUBA diving, practical choices for various design parameters are exemplified as follows:

distance between crystal and wall -- 1 cm
frequency of ultrasound -- 10 MHz

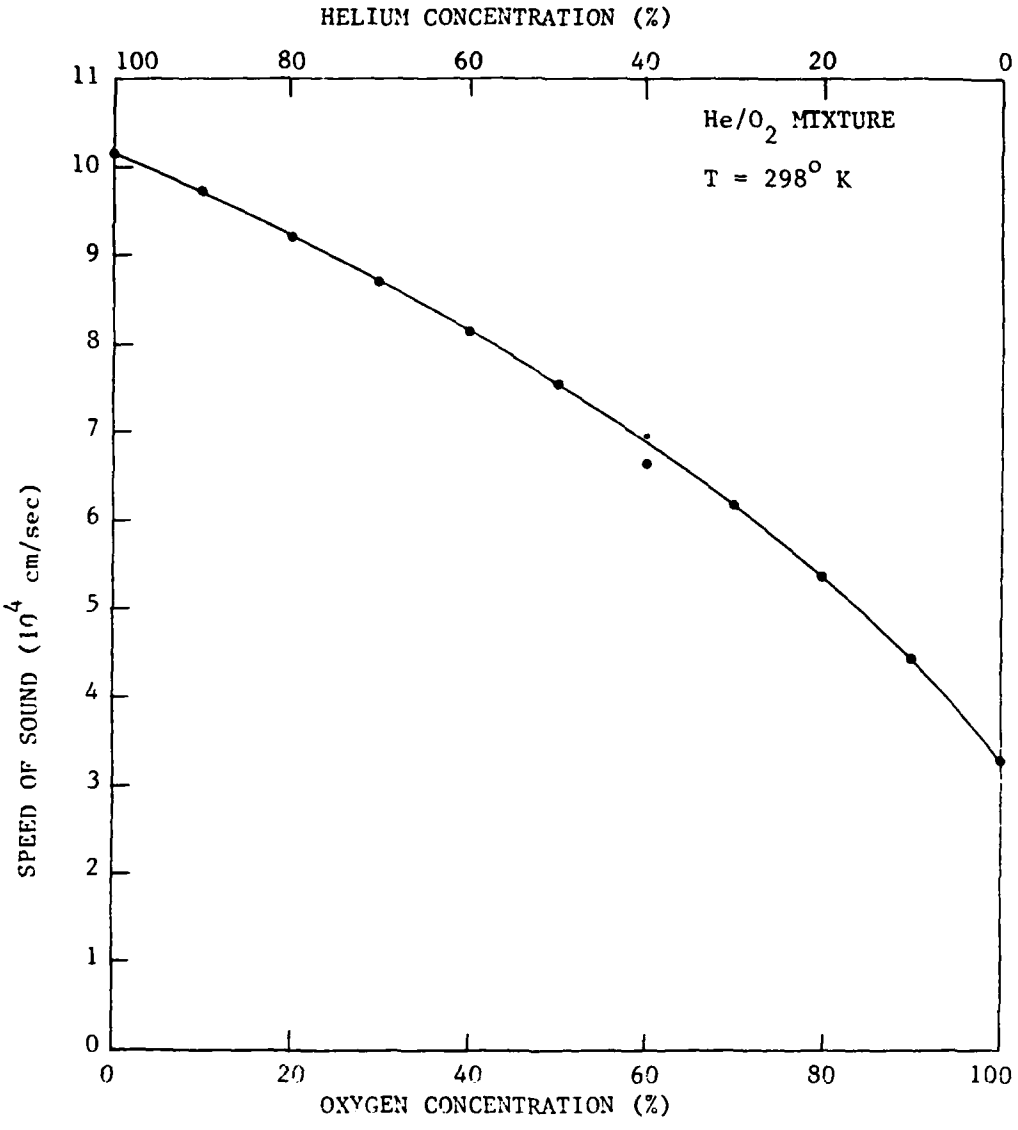

FIGURE 13. SPEED OF SOUND VERSUS HELIUM/OXYGEN CONCENTRATION.

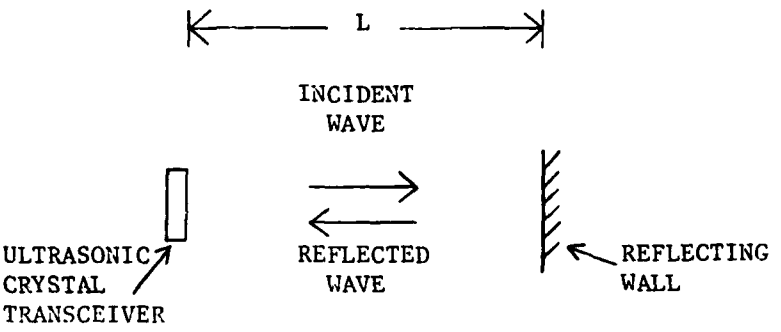

FIGURE 14a. SCHEMATIC DIAGRAM OF AN ULTRASONIC HELIUM SENSOR.

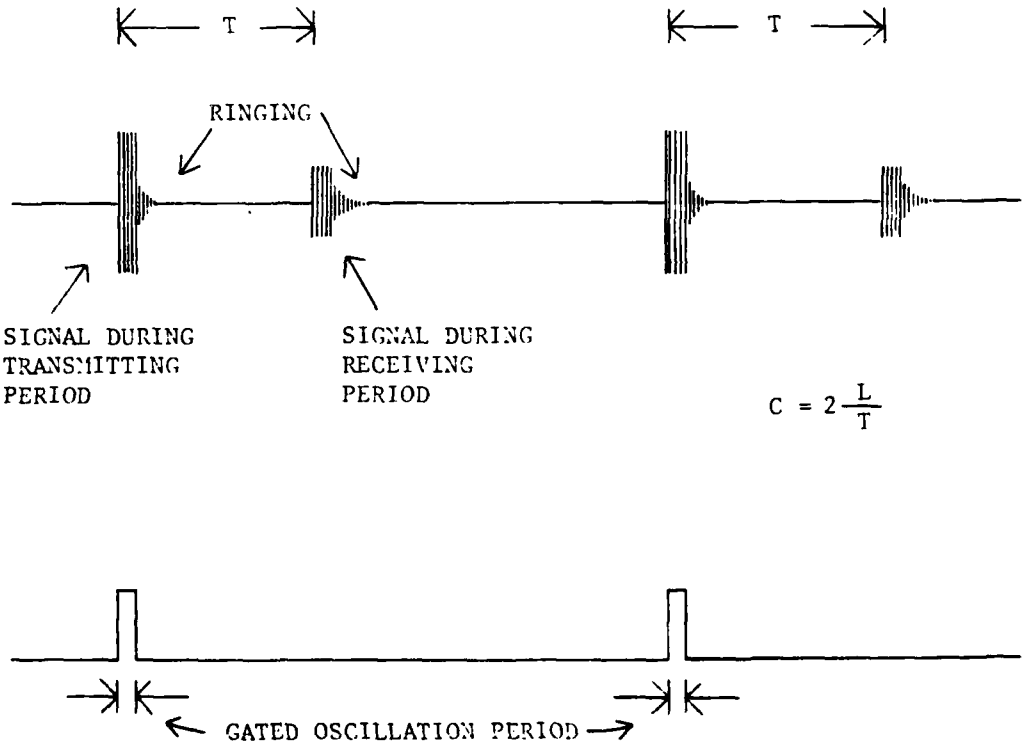

FIGURE 14b. TRANSIT TIME.

FIGURE 14. ILLUSTRATION OF THE TRANSIT TIME MEASUREMENT SCHEME.

Based on these parameters, the shortest transit time corresponding to the case of 100% He is approximately 20 μsec, a magnitude quite measureable by the state-of-art electronics. At 10 MHz, the ultrasound behaves like a beam so that interference of echoes from side walls is not serious. Tuned circuits, filters, time gates and other standard design techniques will add to the accuracy and reliability of the system. Higher frequency (15 MHz, for instance) and larger separation distance will also improve the measurement accuracy of the system.

The ultrasonic helium sensor has not been carried to a stage where actual measurements can be made in the present development.

3.0 CARBON DIOXIDE SENSOR

The CO_2 sensor under current development is an electrolytic anion exchange cell operating in a CO_2 diffusion-limited mode where the cell current is proportional to the partial pressure of carbon dioxide.

The conventional CO_2 sensor uses a pH probe to measure the concentration of hydrogen ion produced when CO_2 is hydrated. The popular Severinghaus pCO_2 electrode (Ref. 4) consists of a standard glass pH electrode covered with a Teflon membrane. Between the glass surface and the membrane exists a thin film of dilute sodium bicarbonate solution. After diffusing through the membrane, CO_2 becomes equilibrated with the electrolyte solution. The pH of the solution is measured by the glass electrode and it can be interpreted in terms of pCO_2 on the basis of the linear relationship between log pCO_2 and pH as described by the Henderson-Hasselbalch equation.

The Severinghaus electrode is not suitable for underwater application due to the following reasons:

1) The pH value is determined in terms of the potential developed by the glass pH electrode. Because this potential is generated by the diffusion of relatively few hydrogen ions across the insulating glass membrane, the glass electrode has a very high internal impedance generally in excess of 200 M ohms. These high impedance characteristics creates a difficult sealing problem underwater.

2) The glass pH probe renders the Severinghaus electrode relatively fragile, bulky, therefore impractical for SCUBA diving.

3) Conventional CO_2 electrodes are very sensitive to temperature due to changes in properties of the glass membrane, in equilibrium constant of the CO_2 hydration reaction, and most importantly, in the electrochemical process.

4) Conventional CO_2 electrodes have a great tendency to drift (even under thermostatic control) and frequent calibration is required.

Therefore, it is obvious that there is a need for a compact, stable, rugged CO_2 sensor suitable for underwater application. The sensor under

development is described in sections to follow.

3.1 Preliminary Study

In electrochemistry, a diffusion controlled current measurement is in general more reliable than a potential measurement. The diffusion process is a well understood phenomenon and the temperature variation of the diffusion coefficient is predictable, reproducible and minute. On the other hand, the development of an electrochemical potential may involve certain obscule, temperature dependent processes relating to electrode surface interaction, activation energy, and microscopic interactions on the molecular level. Therefore, our objective is to devise a method to replace the potential measurement in a conventional CO_2 sensor by a direct current measurement, and in the meantime, cause this current to correspond to the diffusion flux of CO_2 molecules.

A dual half-cell mimicking the functional aspects of a conventional CO_2 sensor is illustrated in Figure 15a. The anodic half cell represents the glass pH electrode which is in effect a perfect cation exchange membrane. The cathode represents the Ag-AgCl reference electrode. The hydrogen ions formed in the CO_2 hydration reaction can pass freely through the cation exchange membrane into the anodic half cell. Because HCO_3^- cannot penetrate the cation exchange membrane, a charge separation will occur, with an excess of HCO_3^- ions near the cathode and an equal number of H^+ ions at the anode. After equilibrium is reached, a constant voltage will be generated. This voltage corresponds to the pH and log $\{pCO_2\}$ of the solution within the cathode compartment.

If the cation exchange membrane in Figure 15a is replaced by a perfect anion exchange membrane, a different voltage of opposite polarity will develop. From symmetry, one can conclude that this voltage will also relate to pH and pCO_2 in a similar manner. The performance of such an anion exchanging cell (Figure 15b) has been investigated and results are summarized in the remainder of this section.

For the diffusion cell shown in Figure 15b, an anion exchange membrane, manufactured by American Machine and Foundry Company of White Plains, NY (type A-100), was interposed between two acrylic half cells by means of clamp-

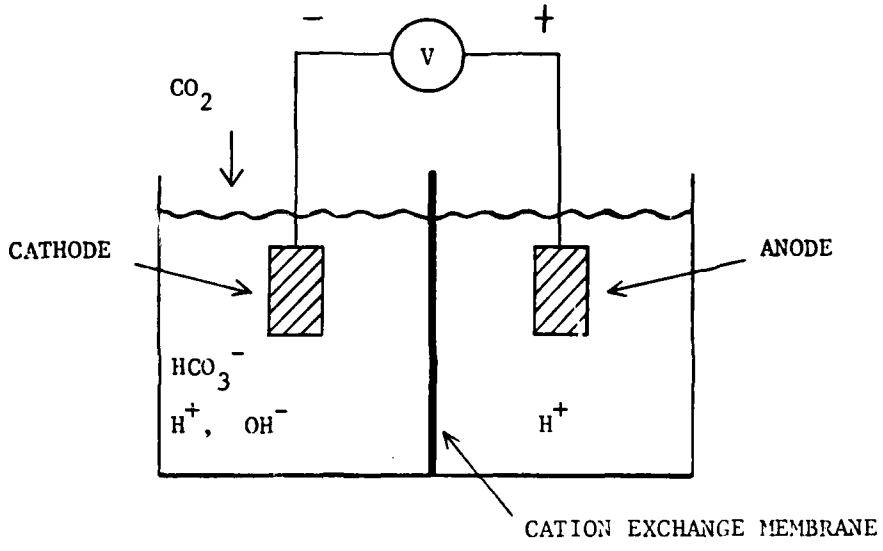

FIGURE 15a. CATION EXCHANGE CELL.

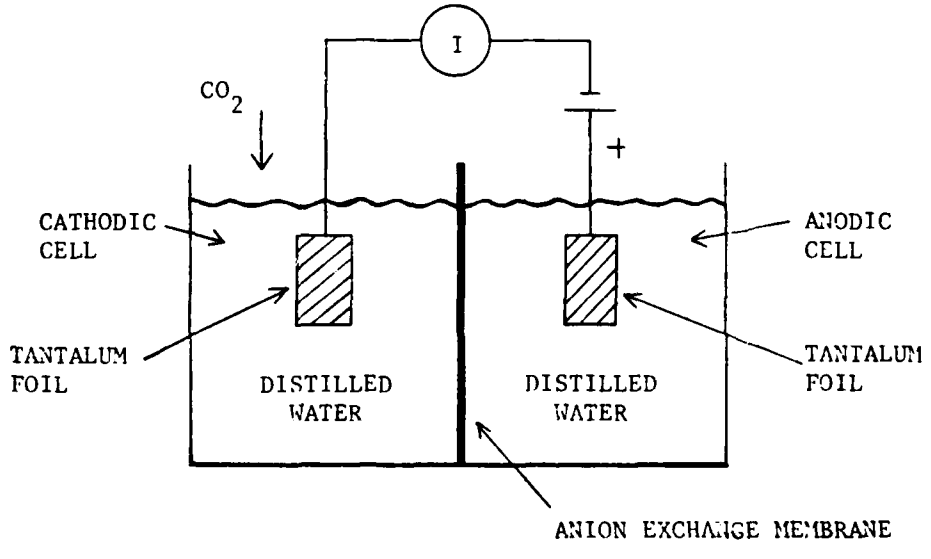

FIGURE 15b. ANION EXCHANGE CELL

FIGURE 15. SCHEMATIC DIAGRAM OF A DUAL HALF-CELL TEST SYSTEM.

ing screws. Two identical tantalum foil electrodes were used as the cathode and the anode. The half cells were individually filled with distilled water and no electrolyte whatsoever was added. Because potential measurements were to be avoided, a constant voltage was maintained between the electrodes and the cell current was measured with a low input impedance (practically speaking, 0 ohm) amplifier. The electrodes were approximately 4 cm apart and were made up of 1 cm x 5 cm tantalum foils (0.013 cm thick) with a tantalum wire spot-welded to one corner.

A 6-Volt battery was used for electrode bias. After an initial surge, the cell current gradually decreased and eventually reached a steady state value of approximately 7 μA. This constant current was believed to be sustained by H^+ and OH^- ions generated by the spontaneous ionization of H_2O.

After initial equilibration, CO_2 was bubbled slowly into the cathodic cell. The cell current increased rapidly, reaching a peak of approximately 250 μA. After the gas was switched off, the current remained at the elevated level for hours and eventually it returned to roughly the original value. The CO_2 induced current is believed to be sustained by H^+ and HCO_3^- ions.

Within the cathodic compartment, the reversible hydration of carbon dioxide occurs spontaneously:

$$CO_2 + H_2O \rightleftarrows H^+ + HCO_3^- \qquad (6)$$

Some of the HCO_3^- ions undergo further ionization:

$$HCO_3^- \rightleftarrows H^+ + CO_3^{--} \qquad (7)$$

The H^+ ions formed are drawn to the cathode and subsequently evolve as hydrogen gas. The anions HCO_3^- and CO_3^{--} are drawn through the anion exchange membrane and react at the anode to form O_2 and CO_2:

$$4\ HCO_3^- \rightarrow 4\ CO_2 + 2\ H_2O + O_2 + 4\ e \qquad (8)$$

$$2\ CO_3^{--} \rightarrow 2\ CO_2 + O_2 + 4\ e \qquad (9)$$

The CO_2 gas released at the anode may very well be rehydrated to form H^+, HCO_3^- and CO_3^{--} ions within the anodic compartment. Because of the large potential gradient exists across the anion exchange membrane, HCO_3^- and CO_3^{--} ions are prevented from returning to the cathodic compartment.

After completion of the previous test, the half cells were evacuated and replaced with fresh distilled water. Following initial equilibration, CO_2 was introduced to the anodic cell instead. The response of the test cell became entirely different. There was only an insignificant and gradual rise in the cell current (2 to 3 μA). The small increase in the cell current is believed to be due to a slight increase in the conductivity of the water within the anodic compartment resulting from formation of H^+, HCO_3^- and CO_3^{--} ions.

It appears that in the test cell of Figure 15b, CO_2 is continuously transported across the anion exchange membrane in such a manner that the CO_2 flux is proportional to the cell current. Therefore, a CO_2 sensor can be devised based on the test cell of Figure 15b. To function as a CO_2 sensor, a diffusion barrier must be provided so that the cell current can become CO_2 supply limited.

3.2 Anion Exchange CO_2 Sensor

Carbon dioxide sensors based on the anion exchange principle have been devised, constructed and tested. These sensors were a scaled down version of the test cell shown in Figure 15b with an additional homogeneous (i.e., non-porous) polymeric membrane serving as a CO_2 diffusion barrier.

3.2.1 Sensor Construction

The construction and the basic monitoring circuitry of the sensor is schematically represented in Figure 16 with gaskets, retaining screens and protective separators omitted. The various functioning layers are:

A) CO_2 Diffusion Membrane
   Material: Dimethyl silicone rubber, 0.0013 cm thick
   Source: General Electric Company, Schenectady, N.Y.
   Function: Diffusion barrier for CO_2 molecules

B) Cathode (Sensing Electrode)
   Material: Porous gold-black
   Source: Engelhard Industries, Carteret, N.J.
   Function: Reduction of hydrogen ions

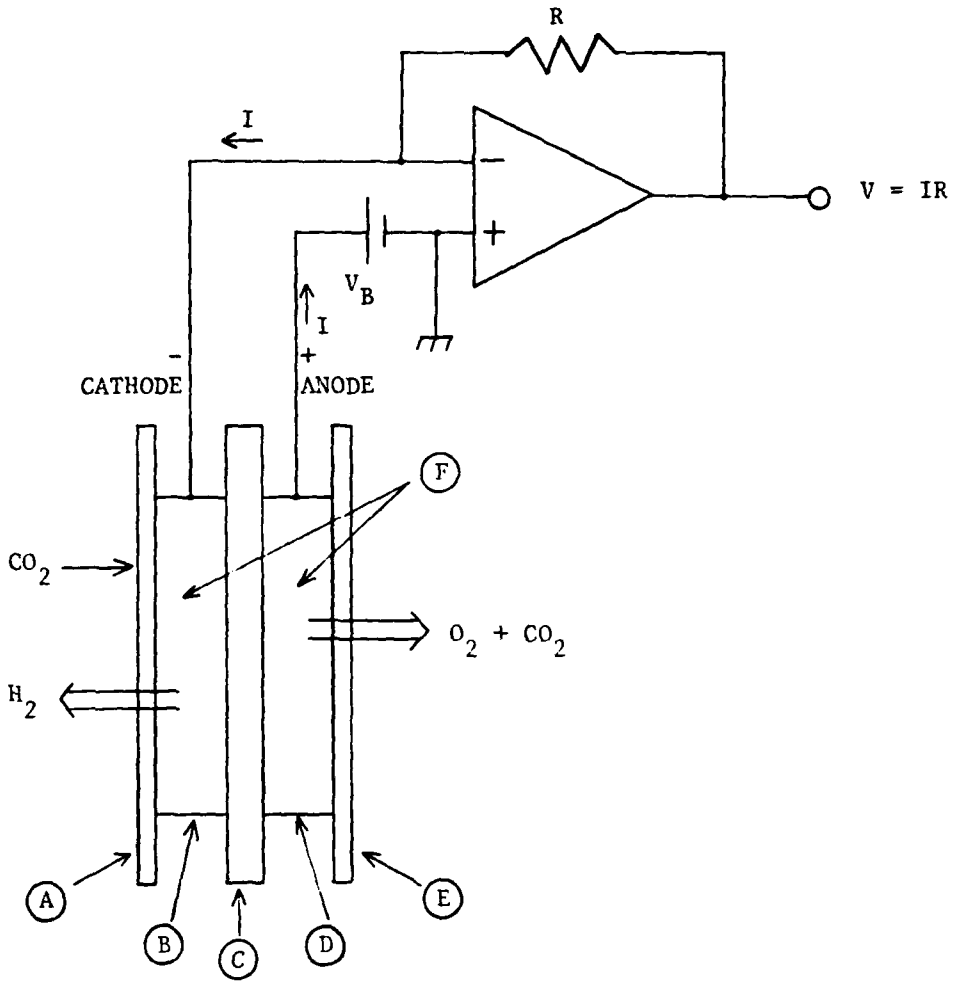

A: CO_2 DIFFUSION MEMBRANE
B: CATHODE (Sensing Electrode)
C: ANION EXCHANGE MEMBRANE
D: ANODE (Counter Electrode)
E: EXHAUST MEMBRANE
F: ELECTROLYTE

FIGURE 16. SCHEMATIC DIAGRAM SHOWING THE CONSTRUCTION AND THE BASIC CIRCUITRY OF AN ANION EXCHANGE CO_2 SENSOR.

C) Anion Exchange Membrane

Material: A-100 exchange resin

Source: American Machine and Foundry Company, White Plains, N.Y.

Function: Selective passage of anions

D) Anode

Material: Porous gold-black

Source: Engelhard Industries, Carteret, N.J.

Function: Neutralization and oxidation of anions

E) Exhaust Membrane

Material: Dimethyl silicone rubber, 0.0013 cm thick

Source: General Electric Company, Schenectady, N.Y.

Function: Discharge of reaction products CO_2 and O_2

F) Electrolyte

Material: 100 mg% solution of carbonic anhydrase enzyme (100 mg enzyme in 100 cm^3 of distilled water)

Source: Sigma Chemical Company, St. Louis, MO, catalog no. C7500

Function: Transport of ions

After passing through the diffusion membrane (Figure 16), CO_2 molecules immediately dissolve in the solution and are subsequently hydrated through the reversible catalytic action of the carbonic anhydrase enzyme. The enzymatic reaction is believed to be as follows (Ref. 5):

$$CO_2 + H_2O \xleftrightarrow{\text{carbonic anhydrase enzyme}} HCO_3^- + H^+ \qquad (10)$$

As reported in Ref. 5, the molecular weight of the enzyme is approximately 30,000, whereas the reaction rate is on the order of 620,000 CO_2 molecules hydrated per enzyme molecule per second.

The H^+ ions generated will be drawn to the cathode electrostatically to evolve as hydrogen gas. On the other hand, the HCO_3^- anions will be drawn through the anion exchange membrane and reacts at the anode to form CO_2 and O_2. The reaction products O_2 and CO_2 can be discharged by diffusion through the exhaust membrane. Some of the CO_2 may rehydrate and remain

in the anodic compartment. The anion exchange membrane allows passage of HCO_3^- ions but prevents CO_2 gas from returning to the sensing cathode compartment. The backward migration of HCO_3^- ions is prevented by the large potential gradient existed across the anion exchange membrane.

Because the enzymatic hydration reaction is extremely fast, the diffusion transport of CO_2 molecules can become the rate determining step. As a result, the cell current becomes CO_2 diffusion-limited and is, therefore, linearly proportional to the partial pressure of carbon dioxide outside the sensor.

3.2.2 Test Results

CO_2 sensors based on the functional design of Figure 16 have been investigated. The sensors were assembled in a layer-by-layer fashion using simple jigs and fixtures. The various layers were held together by two stainless steel end plates and clamping screws. The active area of the sensor, which is determined by the openings in the end plates and the diameter of the cathode, is roughly 0.25 cm in diameter. The various layers in Figure 16 (with the exception of the cathode and the anode) are 0.8 cm in diameter, whereas the end clamping plates are 1.9 cm in diameter. The cathode and the anode were pre-soaked in the enzyme solution and were kept wet all through the assembly procedure. The elctrode lead wires consisted of Teflon coated gold wire 0.013 cm in diameter, which were stripped and pressed against the cathode and the anode, respectively. After assembly, the sensors were rinsed in distilled water to remove traces of enyzme solution external to the sensor.

Gaskets used for sealing were composed of polyethylene disks and rings. The fragile diffusion membranes were protected by thin sheets of hydrophobic, micro-porous polypropylene material. The overall thickness of the sensor is less than 0.4 cm.

After initial equilibration, the sensors were tested in a carbon-dioxide/helium test system composed of flowmeters, check valves, flow restrictors and mixing valves. The electrode bias was provided by a variable voltage power supply at a setting of 2 Volts. The sensor current was monitored by a current amplifier with a front-end current-to-voltage convertor identical

to that of Figure 16. The test results of a typical sensor are presented in Figure 17. The current corresponding to zero pCO_2 was 0.9 μA and the sensor deviated from a linear response for pCO_2 values above 200 Torr. The sensor current became saturated for pCO_2 above 400 Torr., approximately.

Sensors have also been tested with premixed calibration gases. Data shown in Figure 18 were obtained with the use of room air and calibration gases bottled by the London Company of Cleveland, Ohio.

The response time of the sensor has been measured by switching from room air to premixed gas containing CO_2, and then back to room air after a steady state is reached. The characteristic response time, defined as the time to reach 63% of the steady state value, was found to be 5 seconds for increasing pCO_2 and 6 seconds for decreasing pCO_2 (Figure 19).

The long term stability of the pCO_2 sensor has been evaluated. The sensor was tested once a day for nine (9) days with the use of a calibration gas mixture containing 5% CO_2, 12 % O_2 and balance nitrogen. The sensor did not show any definite trend of upward or downward drift, however, it did show slight daily variations (Figure 20). The sensor was continuously biased during the long term study and it was constantly wrapped in a wet towel to keep it from drying out. The sensor reported was still functioning at the present writing.

3.2.3 Carbon Dioxide Sensor Characteristics

The various aspects relevant to the performance and design of the sensor will be discussed in this section.

(1) Linearity

The sensor current was found to be linear with respect to pCO_2 only for values below 200 Torr. (Figure 17). In diving as well as in most biomedical applications, the pCO_2 range of interest rarely exceeds 100 Torr. Nevertheless, the reason for signal saturation was explored. Insufficient enzyme activity as the cause for saturation was ruled out because the linearity range of sensors constructed of different enzyme concentrations had been similar.

The reason for saturation was found to be due to insufficient voltage

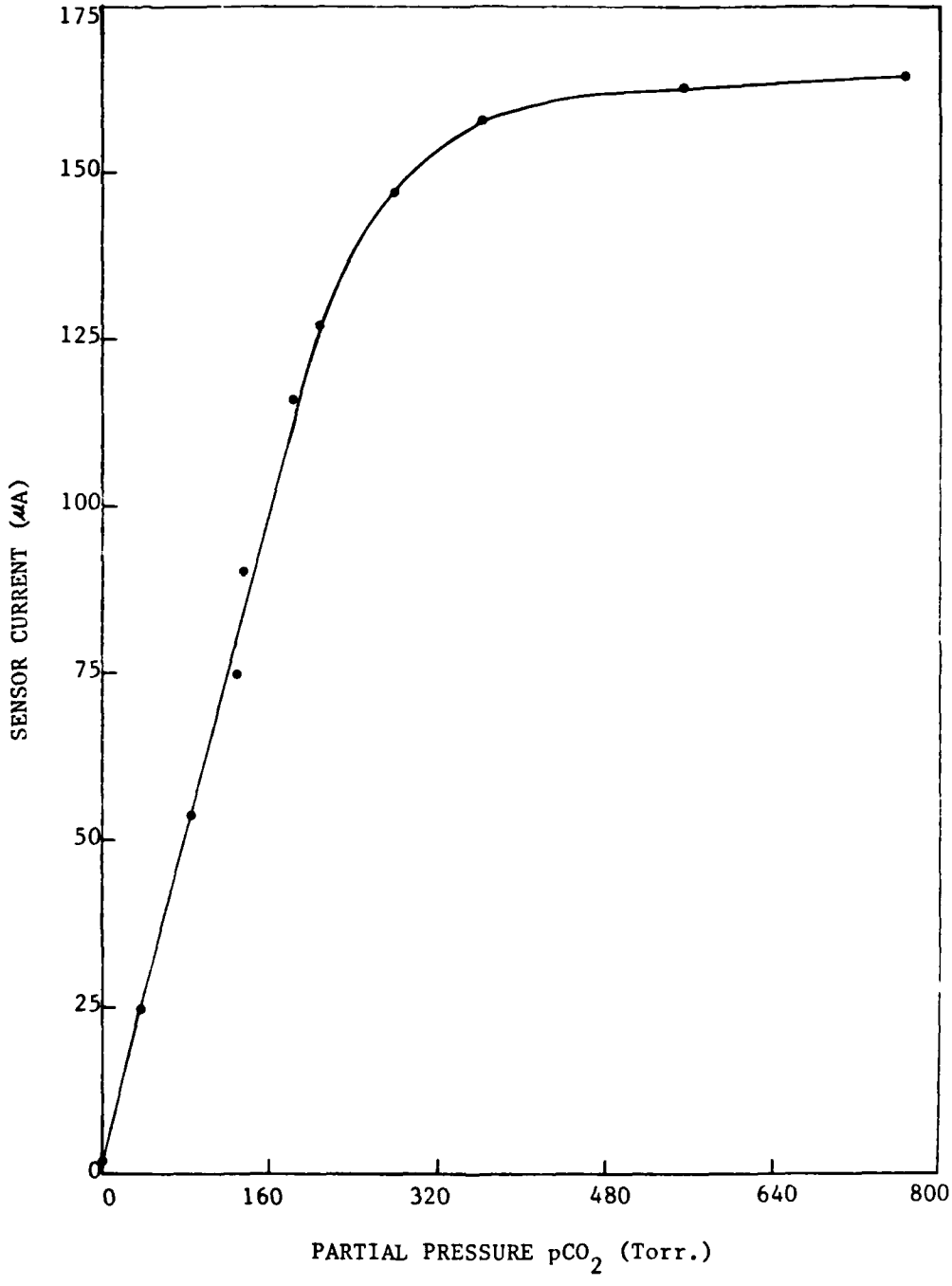

FIGURE 17. SENSOR CURRENT VERSUS CO_2 PARTIAL PRESSURE IN CO_2/H_e GAS MIXTURES.

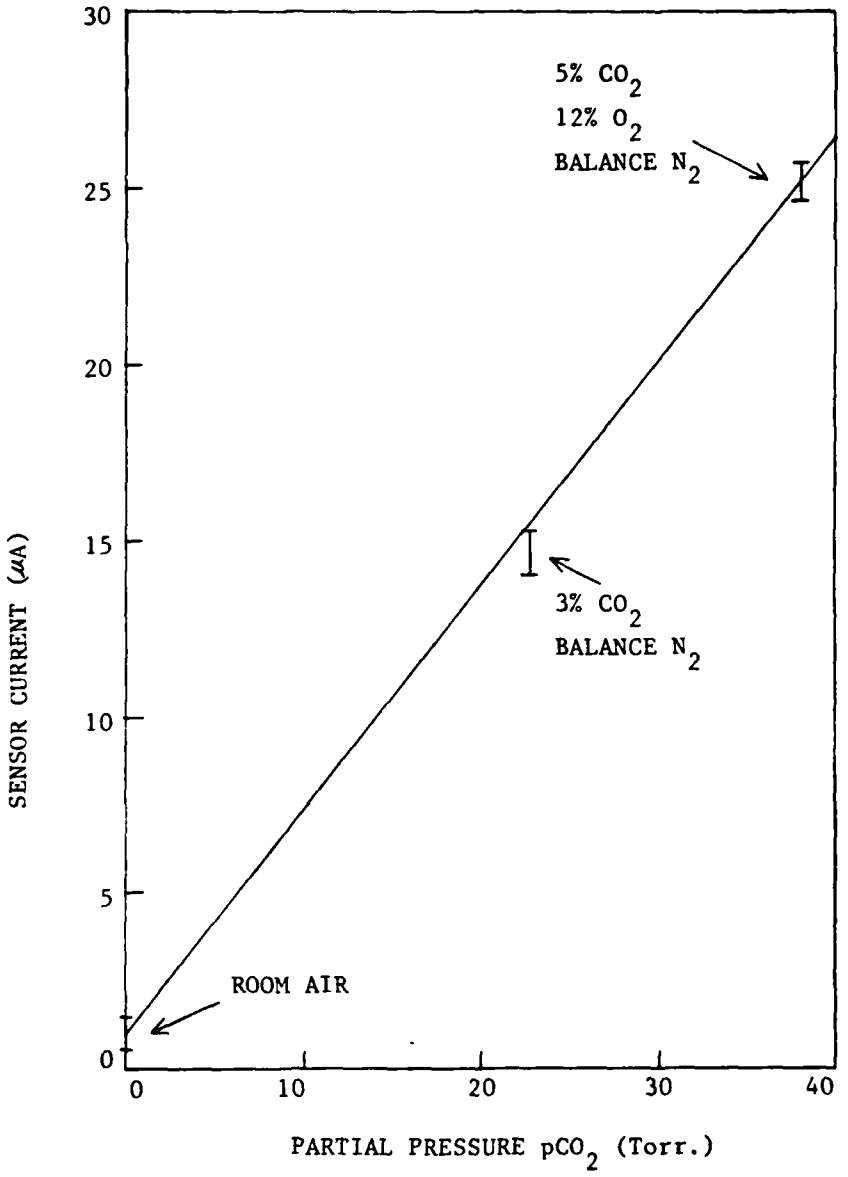

FIGURE 18. CALIBRATION OF pCO_2 SENSOR BY USING PRE-MIXED GAS MIXTURES.

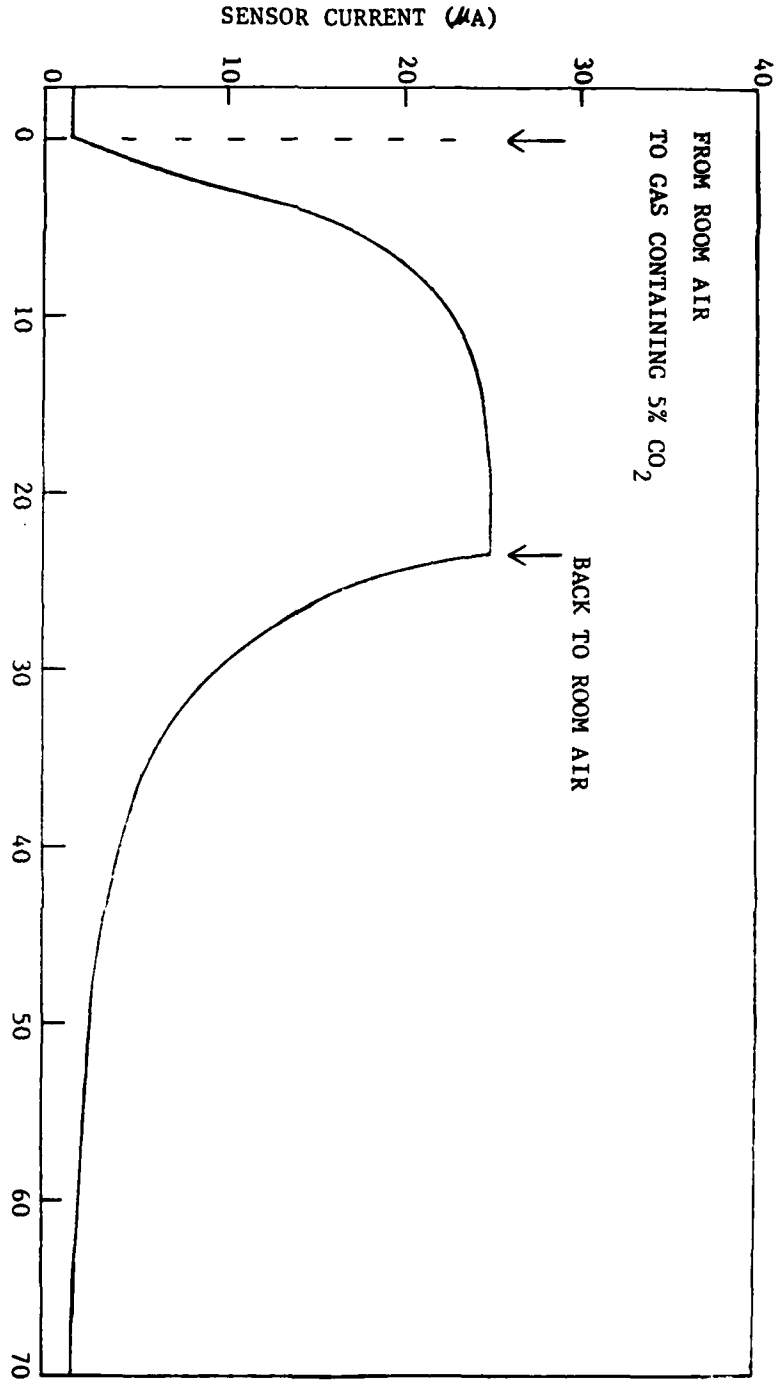

FIGURE 19. RESPONSE TIME OF THE pCO_2 SENSOR.

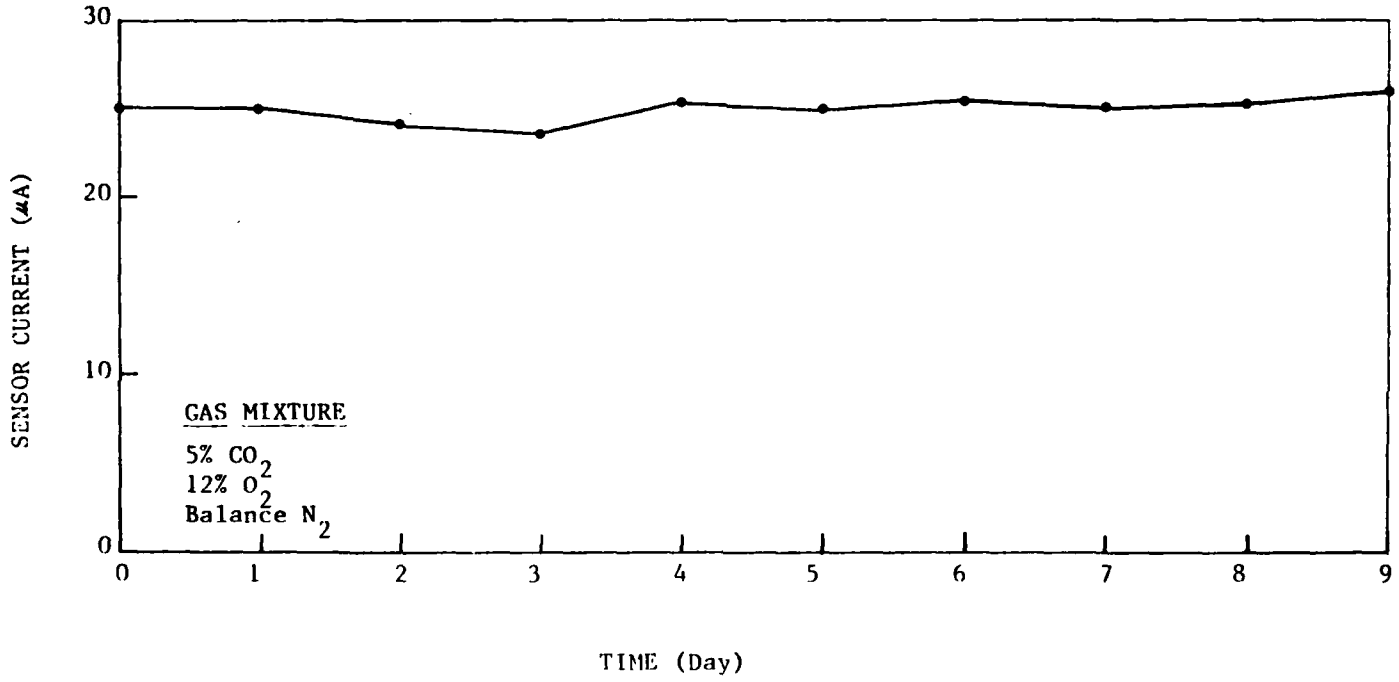

FIGURE 20. LONG TERM STUDY OF pCO_2 SENSOR.

bias. At high concentrations of CO_2, the cell current becomes so large that only a portion of the ions can be collected. It was found that operating the sensor at 6 Volts bias (instead of 2 Volts) extended the linear range to 450 Torr. approximately. However, the sensor degraded rapidly and the anion exchange membrane changed from the normal brown color into black color discovered upon post mortem examination. It appears that the high current density encountered at high pCO_2 had exceeded the performance limit of the anion exchange membrane.

Therefore, the sensor can be rendered linear over a wider dynamic range only by using a diffusion barrier less permeable to CO_2. The penalty for such an approach lies in a lengthening of the response time. As stated earlier, the lack of linearity at high pCO_2 does not in any way detract the usefulness and attractiveness of the sensor in diving as well as in biomedical applications.

(2) Oxygen Sensitivity

In theory, when the potential of the cathode reaches the level of oxygen reduction potential (0.4 Volt in basic solution and 1.23 Volt in acidic solution, relative to standard hydrogen electrode), a current due to electrochemical reduction of O_2 to hydroxyl ion can occur. For the sensor used to obtain the data shown in Figure 18, the sensor current at pO_2 = 760 Torr. was found to be only 2.1 μA. The low sensitivity to oxygen can be attributed to the following factors:

(a) For the dimethyl silicone rubber membrane used, the permeability coefficient of O_2 is 5.4 times smaller than that of CO_2.

(b) The bulk of the potential drop was due to the anode, distilled water, and the anion exchange membrane so that the potential impressed on the cathode is relatively small.

(c) Within the pores of the cathode, the solution tends to be acidic due to the presence of H^+ resulting from CO_2 hydration. As a result, a higher potential is needed for oxygen reduction.

Gold-black is a superior electrode catalyst for O_2 reduction. The choice of porous gold-black as the anode material in the present pCO_2 sensor was

largely due to non-availability of other more suitable materials. It is possible that materials, such as tantalum, cadmium, nickel, chromium and tungsten, can be used as a cathode in order to further reduce the oxygen sensitivity. Incidentally, tantalum screen and foil was found to be unsuitable as an anode material. Rapid degradation perhaps due to the oxidation effect of OH^- ions, had rendered the sensor insensitive to pO_2 in a few days when a tantalum anode was used.

(3) Enzyme Stability

Commercial preparation of the carbonic anhydrase enzyme is known to be stable for more than a year at 5°C. Data on its stability at other temperatures have not been found in the literature. Because the enzyme is an animal (or plant) protein, addition of noninhibiting fungicide/bactericide may be required. On the other hand, the growth problem may be non-existent due to the low pH values encountered. Alternatively, the sensor interior may be sterilized by subjecting to 100% CO_2 (i.e., low pH) initially (at open circuit to avoid large current surge).

Sensors without enzyme have also been constructed and investigated. The variation of sensor current with pCO_2 is shown in Figure 21. As expected, the cell current is considerably smaller.

(4) Offset Current

In addition to the slight sensitivity to oxygen, the pCO_2 sensor has a small but non-vanishing current at zero pCO_2. This offset current is due to impurity in the solution, and more importantly, due to the spontaneous ionization of H_2O molecules. In 100% Helium, this offset current is less than 1 μA, in general (Figure 17).

(5) Service Life

Because water is being consumed, the life span of the sensor is not unlimited. Based on water consumption calculations, the service life of the sensor was estimated to be 10 to 20 days for continuous operation at a pCO_2 level of 40 Torr. The life of the sensor can be extended by using a less permeable diffusion membrane.

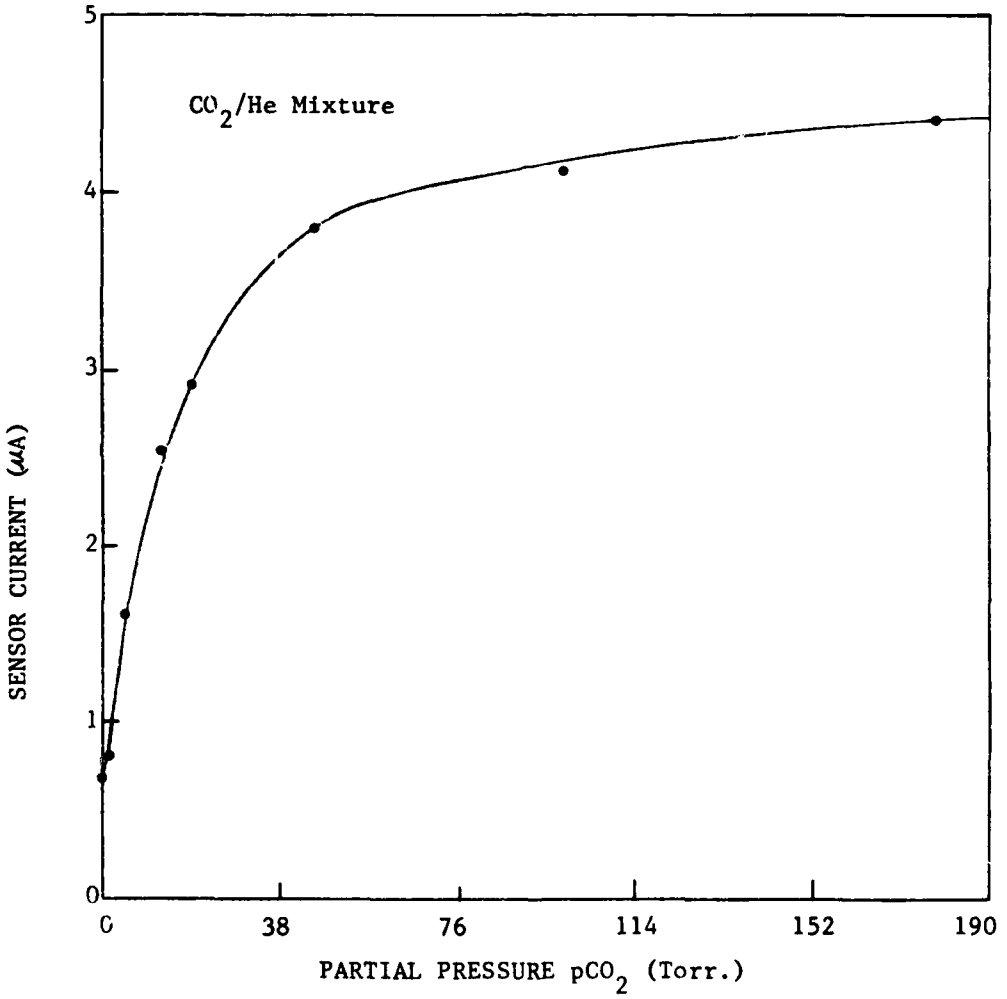

FIGURE 21. CELL CURRENT RESPONSE OF AN ENZYMELESS SENSOR.

(6) Response Time

The response time of the pCO_2 sensor is typically on the order of 5 seconds (Figure 19). A sensor of this performance can already be used in a rebreather type SCUBA system to warn of dangerous elevations of the CO_2 concentration.

(7) Underwater Operation

Because the sensor directly responds to pCO_2, it is readily operable under water with the same calibration as at sea level. Both sides of the sensor can be exposed to the same gas medium to be monitored.

(8) Failure Mode

The CO_2 sensor has been destructively tested by allowing it to dry out. Upon failure, the sensor current fluctuated wildly at relatively high frequency reflecting the random variations of the wetted cathode surface. This distinctive sign of failure is very obvious and unmistakable to any observer.

4.0 FUEL CELL HYDROGEN SENSOR

The sensor under current development is a hydrogen fuel cell operating in a diffusion-limited mode where the short circuit cell current is linearly proportional to the partial pressure of hydrogen. In order to elucidate the subtleties and advantages of the proposed fuel cell sensor, a discussion of the conventional polarographic type sensor is presented.

4.1 Polarographic Hydrogen Sensor

A typical polarographic sensor (Figure 22) consists of a glass-insulated platinum anode resting against a hydrogen-permeable polyethylene membrane. The outer jacket of the electrode consists of an insulating tube which serves as a reservoir for an electrolyte solution composed of KCl. Immersed in the electrolyte is a silver-silver chloride reference cathode. A constant potential difference of 0.4 to 0.5 Volts is maintained between the anode and the cathode. The current flowing between the electrodes is, in general, hydrogen diffusion-limited, and it is therefore linearly related to the hydrogen partial pressure outside the membrane.

The polarographic hydrogen sensor is subject to constant drift and instability due to the following possible causes:

(1) Polarizing potential - The anode potential has to be high enough to oxidize H_2 readily and to minimize the reduction of O_2 which can also reach the anode. Yet the anode potential has to be low enough to minimize the oxidation of hydroxyl ions to O_2, and the dissolution of platinum by forming $PtCl_4^{--}$ and $PtCl_6^{--}$. The existence of such a critical relationship with regard to the polarizing voltage is deplorable.

(2) Offset current - Because a polarizing potential is constantly applied, there is an offset current (I_o in Figure 22) resulting from ohmic conduction in the electrolyte even in the absence of hydrogen. As a result, the straight line in the plot of anode current versus hydrogen pressure does not pass through the origin. The presence of a parasitic offset current is troublesome because it is influenced by many factors.

(3) Degradation of the reference electrode - Due to the prevalent offset current, slow oxidation of the reference electrode may occur.

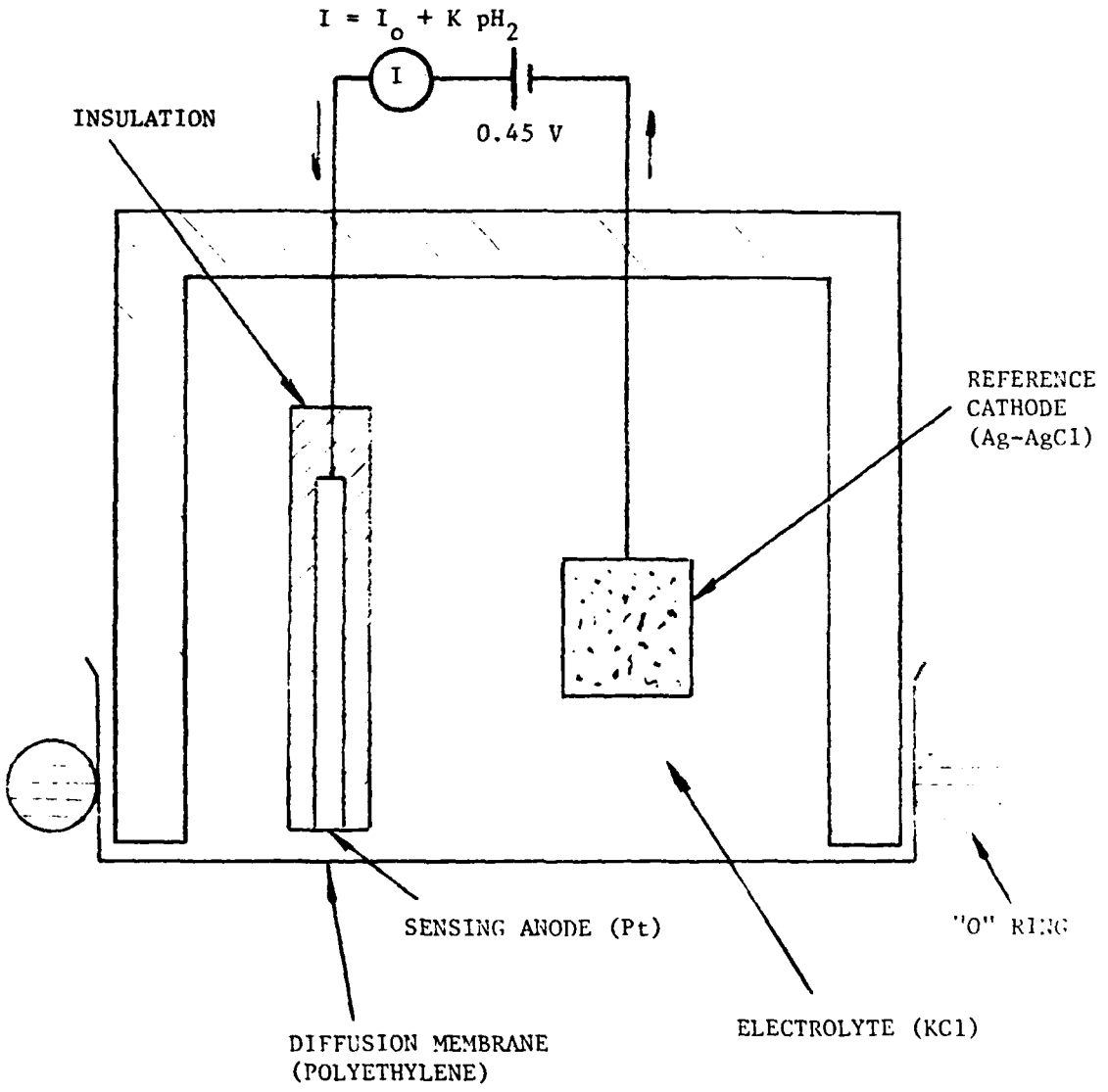

FIGURE 22. A TYPICAL DESIGN OF A POLARGRAPHIC HYDROGEN SENSOR.

(4) Plating of the sensing electrode - Silver ions from the reference electrode may migrate to the sensing electrode.

(5) Variation of anode surface condition - Any conceivable change in the surface condition either due to contamination, variation of monolayer structure, absorption layer, work function, oxide formation, AC or switching transient pick-up may result in a substantial deviation in the hydrogen overvoltage of the metal surface and a noticeable increase or decrease in the sensor signal output which is not mediated through a rise or fall in the hydrogen pressure.

(6) Limitation on electrode area - When an anode of large surface area is used, the zero-hydrogen offset current becomes enormous (relative to the design hydrogen current), and the sensor accuracy and stability is significantly affected. For this reason, the conventional polarographic system cannot take advantage of the high performance porous type catalytic electrode commonly used in power fuel cell construction. Furthermore, with a limited electrode area, any slight contamination of the anode would probably render it electrode-activity-limited so that the hydrogen diffusing into the cell is not completely oxidized, causing the indicated hydrogen partial pressure to be lower than the actual value. The anode to hydrogen diffusion membrane area ratio of polarographic type system is approximately unity.

4.2 Sensor Construction

A fuel cell is an electrochemical energy conversion device designed for generation of electricity by electrochemical oxidation of a fuel and reduction of an oxidant. Since fuel cells can run on hydrogen and oxygen, they can be devised as hydrogen sensors. We have found that using the fuel cell as a quantitative electrochemical instrument has many advantages and merits unmatched by polarographic systems.

The construction of the sensor is schematically shown in Figure 23, with gaskets, retaining layers and protective separators omitted for clarity. The various functional layers are:

A) Hydrogen Diffusion Membrane
   Material: Polyimide film, 0.0008 cm thick
   Source: E.I. duPont de Nemours & Company, Wilmington, Delaware

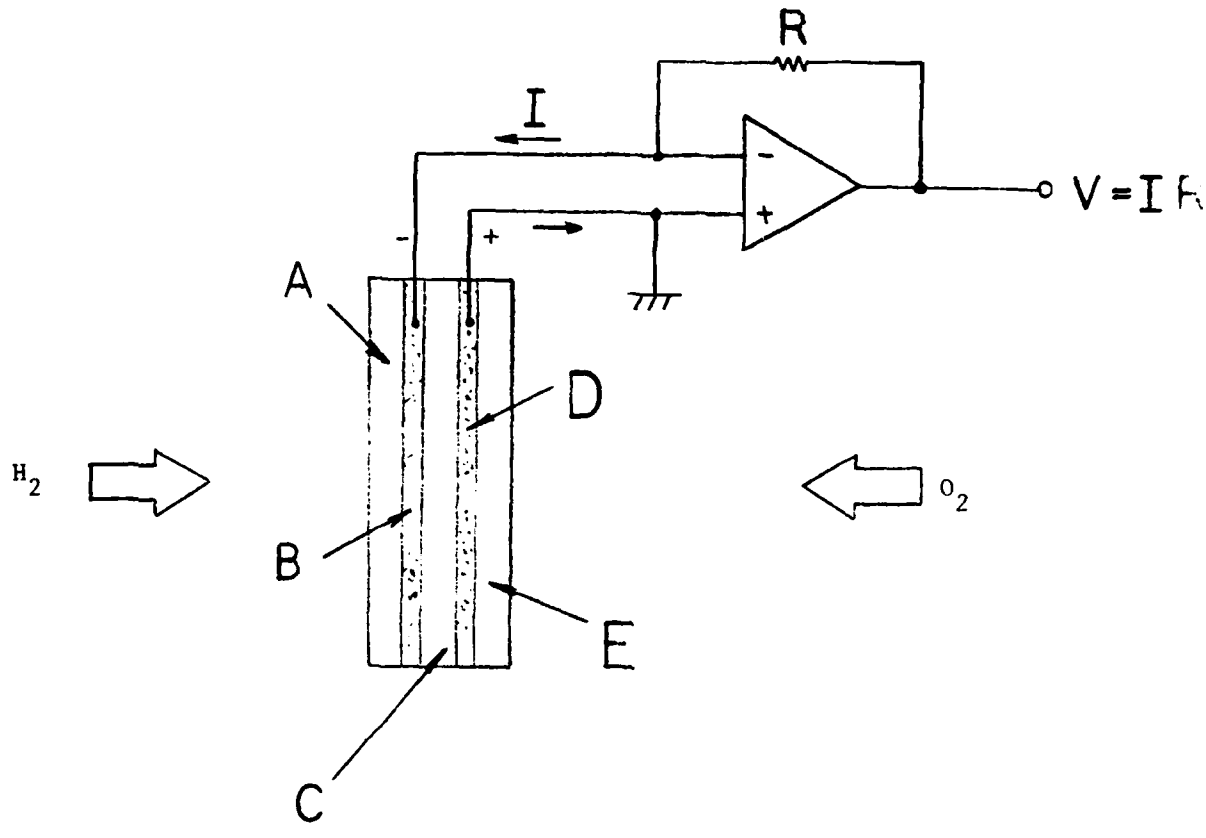

A: HYDROGEN DIFFUSION MEMBRANE

B: ANODE

C: CATION EXCHANGE MEMBRANE

D: CATHODE

E: OXYGEN MEMBRANE

FIGURE 23. FUNCTIONAL DESIGN OF A FUEL-CELL HYDROGEN SENSOR.

Function: Diffusion barrier for hydrogen molecules

B) Anode (sensing electrode)

Material: Platinum-Black

Source: Engelhard Industries, Carteret, N.J.

Function: Electrode catalyst for hydrogen oxidation

C) Cation Exchange Membrane

Material: NAFION perfluorosulfonic acid polymer

Source: E.I. duPont de Nemours & Company, Wilmington, Delaware

Function: Solid electrolyte and divider for the anode and cathode compartments

D) Cathode

Material: Gold-Black

Source: Engelhard Industries, Carteret, N.J.

Function: Creation of an auto-genous polarizing potential for hydrogen oxidation

E) Oxygen Membrane

Material: Hydrophobic membrane, porous polypropylene

Source: Celanese Plastics Company, Newark, N.J.

Function: Supply of oxygen necessary for the reaction

The anode and the cathode were composed of microporous catalysts dispersed in a hydrophobic Teflon binder with a loading of 30 to 40 mg/cm^2. Prior to assembly, the porous platinum-black anode and the porous gold-black cathode were pre-deposited with a thin layer of sulfuric acid by vacuum impregnation. This thin acid layer not only provides a better coupling with the cation exchange membrane but also allows triple-phase reaction sites to exist.

The electrode lead wires were composed of tantalum annular disks on which Teflon coated stainless wires (0.013 cm in diameter) were attached by spot-welding. The inner circular edge of the disk (0.25 cm in diameter) was made to overlap and to contact the electrode at its perimeters. The active area of the sensor was therefore 0.25 cm in diameter. Like the CO_2 sensor, the fuel cell hydrogen sensors were also assembled in a layer-by-layer fashion with no further addition of acid solution. The clamping end

plates used are identical to those for the CO_2 sensor. The overall thickness of the sensor is less than 0.4 cm.

4.3 Principle of Operation

The various electrode reactions can be summarized as follows:

$$H_2 \xrightarrow{Pt} 2H^+ + 2e^- \qquad \text{Anodic Reaction} \qquad (11)$$

$$\tfrac{1}{2}O_2 + 2H^+ + 2e^- \xrightarrow{Au} H_2O \qquad \text{Cathodic Reaction} \qquad (12)$$

$$H_2 + \tfrac{1}{2}O_2 \longrightarrow H_2O \qquad \text{Overall Reaction} \qquad (13)$$

After diffusing through the barrier, the hydrogen molecules enter various pores of the anode and react on the platinum surface. The hydrogen ions generated migrate through the cation exchange membrane and then react with oxygen at the cathode to form H_2O molecules. The sensor current flows from the cathode, via external monitoring circuitry, to the anode. Because of the high open-loop-gain of the operational amplifier (Figure 23), the voltage at the cathode is, for all practical purposes, equal to that at the anode and the cell is therefore under short circuit condition. The current circulating through the cell is directly proportional to the diffusion flux of hydrogen molecules, and is, in turn, proportional to the partial pressure of hydrogen.

4.4 Potential Advantages of Fuel Cell Sensor

The various salient features of the fuel cell sensor design are highlighted as follows:

(1) No Offset Current

The offset current is defined as the parasitic cell current present when the sensor is exposed to a hydrogen-free gas. Because the operation of the proposed sensor is spontaneous and self-sustaining, externally applied voltage is not used, therefore an offset current can never be sustained. As a result, the offset current is non-existent, zero offset current is a common characteristic of fuel cell type sensors.

(2) Single Point Calibration

Because the offset current is always zero, sensor calibration can be

achieved by single check point.

(3) No Restriction on Electrode Area

Unlike the case of a polarographic sensor, there is no restriction on electrode area. Hence, the high performance, porous type electrode can be used and the sensor anode and the cathode are never catalyst-activity-limited. The sensor is therefore extremely insensitive to anode contamination and degradation. The ratio of effective anode area to the apparent area is approximately 3000 (the same ratio in polarographic sensor is approximately 1).

(4) Prevention of Oxide Formation on Anode

Because the internal "polarizing" potential is self-generated and self-regulated by the cathode (as against externally applied voltage), O_2 reduction and oxidation of the hydroxyl ion to O_2 will never happen on the anode. Since oxide will not form on the anode, direct reaction between H_2 and O_2 on the sensing anode surface with no electron trnasfer cannot happen.

(5) *Insensitivity to Electrolyte Concentration*

As long as the internal cell resistance is small the electrolyte concentration has no effect on the hydrogen current. Note that in a polarographic sensor, the electrolyte concentration affects the parasitic offset current and therefore the apparent hydrogen partial pressure.

From the above discussion it is clear that the proposed sensor will be inherently more stable due to the successful elimination of various limitations associated with the polarographic type sensor.

4.5 Test Results

The fuel cell hydrogen sensor has been fabricated, tested and refined. A typical calibration curve is given in Figure 24 with the cathode side exposed to air and the anode side exposed to hydrogen/helium gas mixtures at 1 atm.

For SCUBA diving, the hydrogen/oxygen gas mixture varies from approximately 79%/21% at sea level to almost 100%/0% at great depths. The sensor response at this concentration range has been investigated with the use of

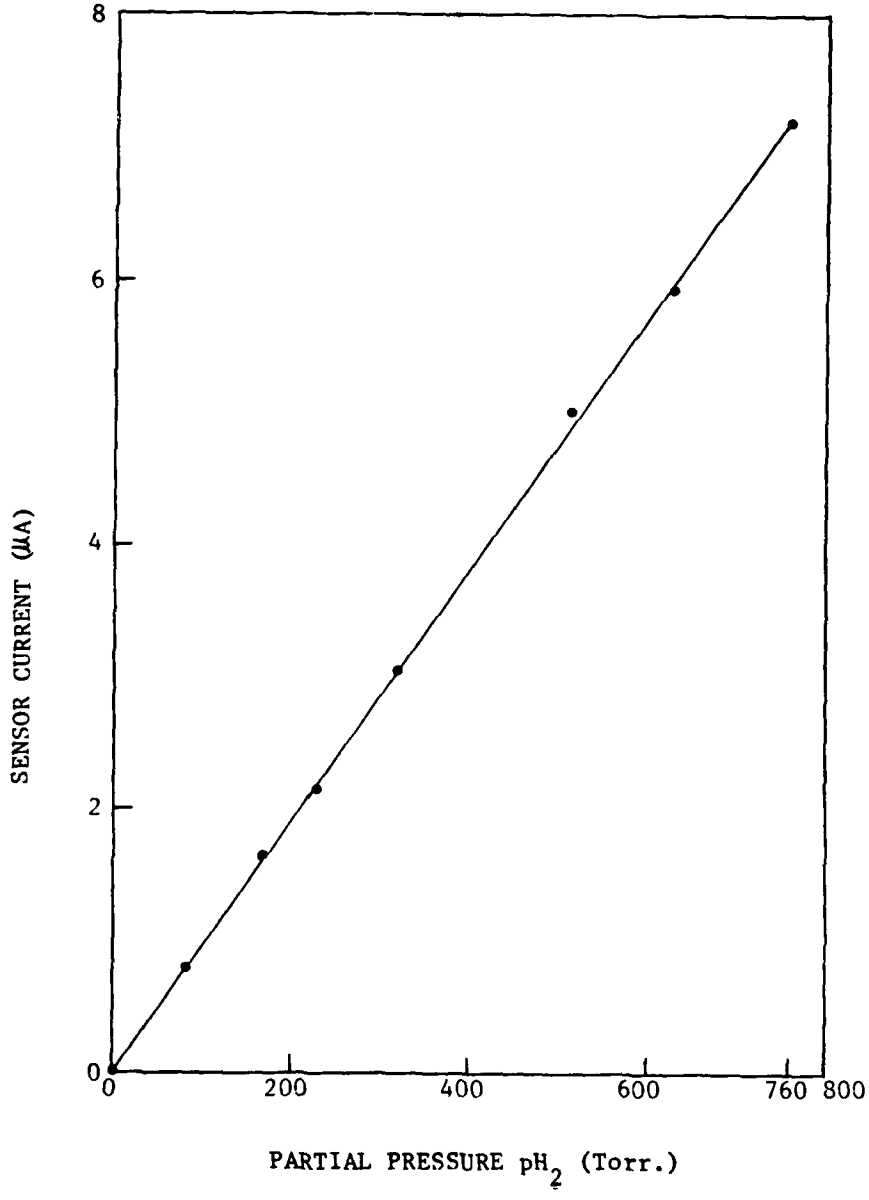

FIGURE 24. SENSOR CURRENT VERSUS pH_2 IN A HYDROGEN/HELIUM MIXTURE.

precalibrated and premixed gases. For safety reasons, argon has been used to replace oxygen. The test results and the standard deviations at different concentrations are given in Figure 25. The gas mixtures were G.C. analyzed containing 100%, 94.85%, 89.7%, 85.6% and 79.8% H_2, respectively. The sample size varies from 5 to 8 at each concentration taken over a time span of approximately 8 hours.

The response time of the hydrogen sensor has been determined by a method involving fast switching from helium to hydrogen and then back to helium. The characteristic response time for ascending and descending hydrogen partial pressure are 3.5 seconds and 5.5 seconds, respectively (Figure 26).

Up to this point, the sensor has been tested with its cathode exposed to room air. In actual application, hydrogen can easily reach the cathode, and it was hoped that its presence can be tolerated due to the low reactivity of the gold cathode towards hydrogen. Contrary to expectations, test results show that the activity of gold-black cathode for hydrogen oxidation is non-negligible.

Therefore, it appears certain that in order to use the hydrogen sensor in underwater applications, only oxygen devoided of hydrogen can be exposed to the cathode. This requirement can be achieved by connecting the cathode compartment to a rubber container or a distensible bag into which oxygen can be injected before diving via a resealable septum.

In summary, test results have shown that:

A) There is no "offset current" and single point calibration will generally suffice.

B) The sensor has a wide dynamic range. Although test at high pressure corresponding to large depths have not been performed, the sensor is expected to retain its linearity through the depth due to the restrictive diffusion barrier used which is evidenced by the small cell current corresponding to pH_2 of 760 Torr. (Figure 24).

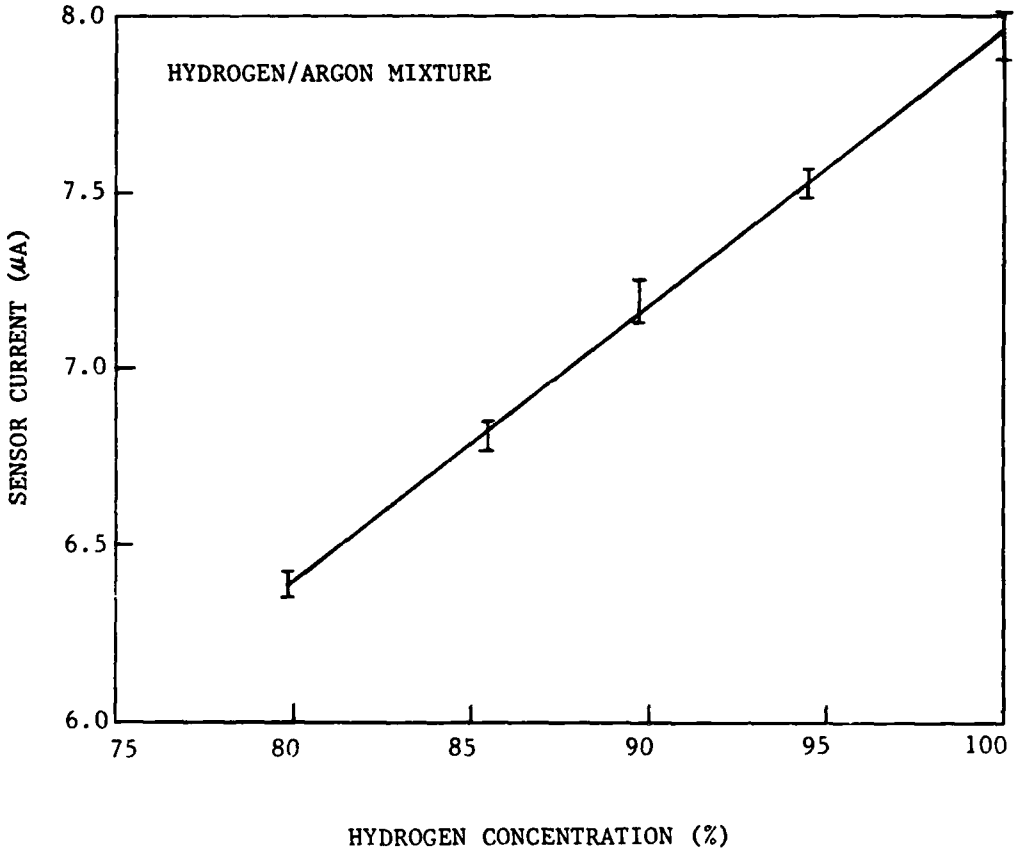

FIGURE 25. CALIBRATION OF HYDROGEN SENSOR USING PRE-MIXED AND ANALYZED HYDROGEN/ARGON GASES.

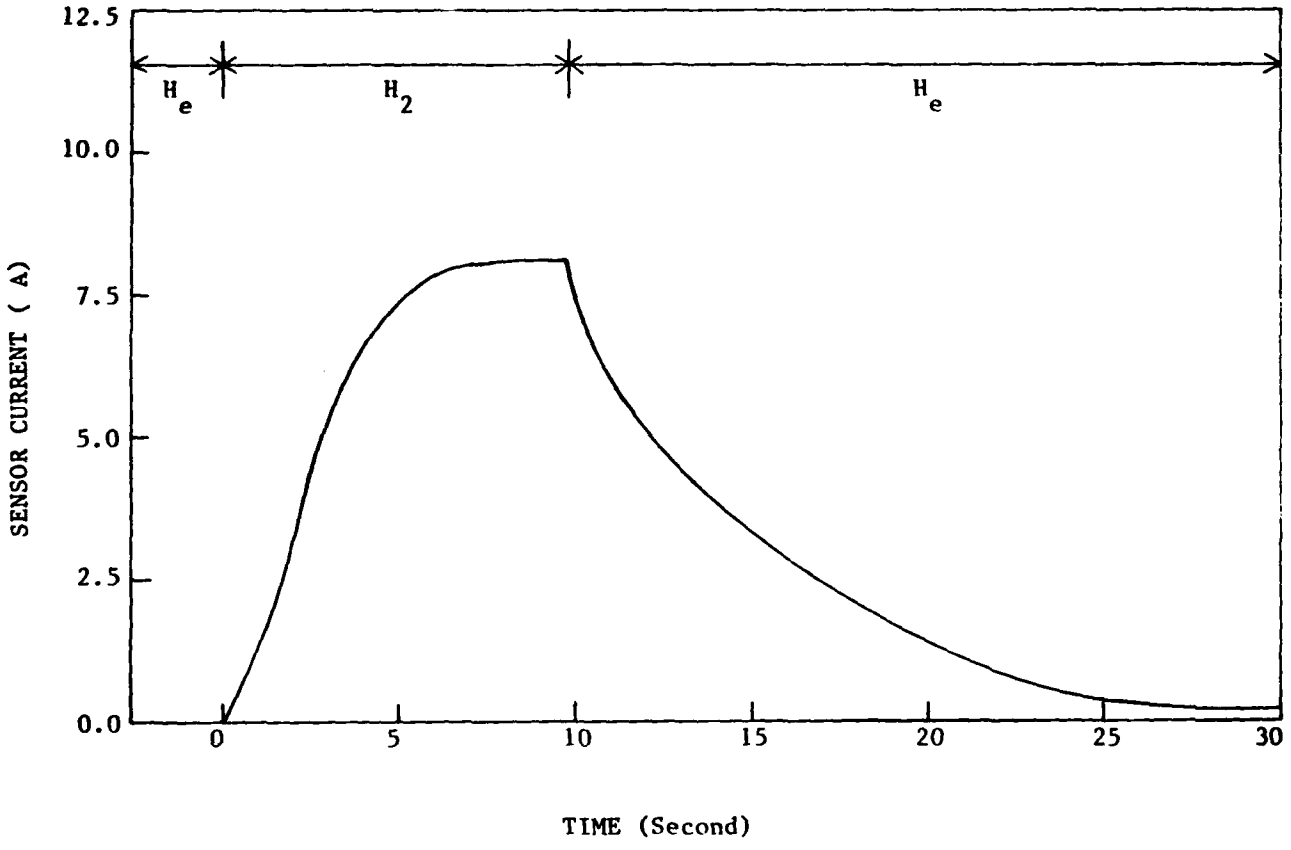

FIGURE 26. RESPONSE TIME MEASUREMENT OF THE HYDROGEN SENSOR.

5.0 CONCLUSIONS

Laboratory versions of the helium, carbon dioxide and hydrogen sensor have been designed, fabricated and tested. Relevant data and underlying principles have been presented in order to allow an assessment of the feasibility and practicality. Due to the multitude of sensors under development and the constraints of time and resources, the characterization and refinement of various sensors is regretably incomplete and nonexhaustive. The progress of the current feasibility phase of the program can be summarized as follows:

(1) Helium Sensor

Two versions of the propsed helium sensor have been investigated, one based on frequency-shift measurement and the other based on amplitude detection. The method based on frequency measurement was found to be ineffective. The method involving amplitude measurement is more reliable, easier to implement and more sensitive. Other salient features include long term stability, reliability, ruggedness and small size. The principle drawback of the amplitude detection helium sensor lies in its sensitivity to hydrostatic pressure. As a result, different calibration curves for different depths must be used.

An alternate method involving speed of sound measurement has been advanced. Based on well-developed theories, the speed of sound is very sensitive to the helium concentration and is a function of temperature, mole fraction, ratio of specific heats and molecular weight of the component gases. The sensor calibration is, therefore, potentially independent of pressure, density and the depth. To date, working models of the speed-of-sound helium sensor have not been constructed, however, its successful development is assured, indeed.

Although not demonstrated, the amplitude detection as well as the speed-of-sound helium sensor are potentially capable of on line, breath-by-breath analysis of the respiration gas. At the very least, the sensor can be used as a monitor, a warning device or for automatic proportioning of the breathing gas in underwater applications.

(2) Carbon Dioxide Sensor

The feasibility and practicality of the enzymatic/electrolyte anion exchange sensor has clearly been demonstrated. The original goal of rendering the sensor current under membrane diffusion control has been achieved. The sensor is compact, fast responding, rugged, sensitive, linear within the range interest and has low offset current. The sensor is potentially stable and long term stability over a 9-day test period has been established. With further development, the proposed sensor may indeed be very useful for CO_2 measurement in a rebreather SCUBA system as well as in biomedical settings. Because of the low level of CO_2 involved, the response time can potentially be reduced to the point where on line, breath-by-breath monitoring is possible.

Because the sensor responds to the partial pressure directly, it can be calibrated at sea level conditions and be used underwater with no further correction other than that due to temperature variation.

(3) Hydrogen Sensor

Like the CO_2 sensor, the feasibility and practicality of the fuel cell hydrogen sensor has been demonstrated, and the sensor current is membrane-diffusion-limited. The sensor has no offset current and single-point calibration will suffice. The sensor responds to partial pressure, has wide dynamic range and is potentially capable of monitoring the enormous hydrogen partial pressure at great depths.

Due to the high flux of hydrogen involved, it is not likely that the response time can be improved to effect direct on line respiration measurements. Nevertheless, it can be devised with a trapping device to measure the end-tidal expired gas sample, in addition to the obvious application in the automatic proportioning of breathing gas at great depths.

6.0 RECOMMENDATIONS

Based on test results, discussions and observations presented in previous sections, the following recommendations are ventured:

Helium Sensor

1) Concentrate effort on the development of the ultrasonic, speed-of-sound type helium sensor in lieu of the less attractive amplitude-detection sensor

2) Develop an automatic underwater breathing gas proportioning system with feedback control by means of the proposed helium sensor

3) Develop an on line, breath-by-breath helium sensor for respiration gas monitoring

Carbon Dioxide Sensor

1) Optimize the design of the proposed sensor with emphasis on diffusion membrane, cathode material and anion exchange membrane

2) Develop a CO_2 warning system for inspired gas monitoring in rebreather type SCUBA system

3) Develop a fast responding, on line, breath-by-breath CO_2 sensor

Hydrogen Sensor

1) Optimize and refine the sensor design with emphasis on diffusion membrane material and the design of a collapsible/refillable oxygen compartment

2) Develop an automatic depth adjusted underwater breathing gas proportioning system using the proposed hydrogen sensor

3) Develop an automatic sensor system for discrete measurement of the expired end tidal gas sample

The desirability and need for the proposed sensors in existing SCUBA systems is obvious. The ability to monitor diluent gas breath-by-breath is also important. Instead of following a universal decompression table, the diver can ascend according to the washout rate measured in his end expiratory samples.

7.0 REFERENCES

1) Lamb, H. Dynamical Theory of Sound Dover Publications, New York, pp. 241 (1935).

2) Pierce, A.D. Acoustics: An Introduction to its Physical Principles and Applications McGraw-Hill Book Company, New York (1981).

3) Rayleigh, J.W.S. The Theory of Sound Vol. 2, Sec. 375, Dover Publications, New York (1945).

4) Severinghaus, J.W. Electrodes for Blood and Gas pCO_2, pO_2, and Blood pH Acta Anaesthesiol. Scand. 6, pp. 207 (1962).

5) Williams, R.J. and Lansford, E.M., Jr. The Encyclopedia of Biochemistry Reinhold Publishing Corporation, New York, pp. 189 (1967).

DISTRIBUTION LIST

22 copies of the Final Report are delivered to the following:

Procurement Contracting Officer — 1 copy
Office of Naval Research
Code 614:CEA
800 North Quincy Street
Arlington, Virginia 22217

Office of Naval Research — 2 copies
Code 441NP
800 North Quincy Street
Arlington, Virginia 22217

Defense Technical Information Center — 12 copies
Cameron Station, Building 5
Alexandria, Virginia 22314

Naval Research Laboratory — 6 copies
Technical Information Division
Code 2627
Washington, D.C. 20375

Commanding Officer, ONREAST — 1 copy
Barnes Building
495 Summer Street
Boston, Massachusetts 02210